

doi: 10.12029/gc20200316

张波,苏尚国,王国栋,司晓博,伍月,蒋校,冯艳芳,刘江涛. 2020. 河北武安洪山正长岩杂岩体中单斜辉石矿物成分特征与岩浆演化过程[J]. 中国地质, 47(3): 782–797.

Zhang Bo, Su Shangguo, Wang Guodong, Si Xiaobo, Wu Yue, Jiang Xiao, Feng Yanfang, Liu Jiangtao. 2020. Mineral chemistry of clinopyroxene from the Hongshan syenite complex in Wu'an, Hebei Province: Implications for magma evolution[J]. Geology in China, 47(3):782–797 (in Chinese with English abstract).

河北武安洪山正长岩杂岩体中单斜辉石矿物成分特征与岩浆演化过程

张波¹, 苏尚国¹, 王国栋², 司晓博¹, 伍月³, 蒋校⁴, 冯艳芳⁵, 刘江涛⁵

(1. 中国地质大学(北京)地球科学与资源学院, 北京 100083; 2. 山东省水土保持与环境保育重点实验室, 临沂大学资源环境学院, 山东 临沂 276005; 3. 中国地质调查局沈阳地质调查中心, 辽宁 沈阳 110034; 4. 中国国土资源航空物探遥感中心, 北京 100083; 5. 中国地质调查局发展研究中心, 北京 100037)

提要:洪山正长岩杂岩体发育较多的具有核-边(核-幔-边)结构的单斜辉石,通过研究单斜辉石成分的变化,可以获得岩石成因及演化信息。本文在详细野外地质调查的基础上,采用锆石U-Pb年代学、矿物学研究,获得洪山正长岩杂岩体内黑云辉石正长岩锆石U-Pb年龄为(126.9±1.2)Ma,是华北克拉通岩石圈减薄峰期的产物;洪山正长岩杂岩体内辉石正长岩与黑云辉石正长岩中单斜辉石Mg#值分别在39.4~72.5、55.4~81.7,具有较高FeO、Na₂O、CaO含量,较低Al₂O₃、MgO、TiO₂含量的特征;单斜辉石总体具有透辉石→霓石的演化趋势,并与熔体达到平衡状态,单斜辉石在初始演化时具有Fe²⁺对Mg²⁺的取代关系,随着演化的进行,岩浆更加富钠、富铁,反映了岩浆体系具有高温、中等氧逸度和富碱的特点。结合单斜辉石核-边(核-幔-边)具有截然的接触关系和不连续的化学组成,表明洪山正长岩杂岩体在形成后还经历了富钠、富铁流体的改造,致使单斜辉石形成了具有富钠、富铁的边部,流体可能是由西向东(或者由洪山正长岩杂岩体中部向外部)对杂岩体进行改造的。

关 键 词:正长岩杂岩体;单斜辉石;矿物学;锆石U-Pb年龄;中生代;岩浆演化;富钠流体;地质调查工程;武安;河北
中图分类号:P578.954 **文献标志码:**A **文章编号:**1000-3657(2020)03-0782-16

Mineral chemistry of clinopyroxene from the Hongshan syenite complex in Wu'an, Hebei Province: Implications for magma evolution

ZHANG Bo¹, SU Shangguo¹, WANG Guodong², SI Xiaobo¹, WU Yue³,
JIANG Xiao⁴, FENG Yanfang⁵, LIU Jiangtao⁵

(1. School of Earth and Resources, China University of Geosciences (Beijing), Beijing 100083, China; 2. Shandong Provincial Key Laboratory of Water and Soil Conservation and Environmental Protection, School of Resources and Environment, Linyi University, Linyi 276005, Shandong, China; 3. Shenyang Institute of Geology and Mineral Resources, China Geological Survey, Shenyang

收稿日期:2020-01-14; 改回日期:2020-02-27

基金项目:国家自然科学基金项目(41272105, 41802201)、中国地质调查局项目(12120115069701、DD20190429)、教育部博士学科点基金(20130022140001)和山东省自然科学基金项目(ZR2018BD012)联合资助。

作者简介:张波,男,1986年生,博士生,从事矿物学、岩石学、矿床学专业; E-mail: zbotdw@163.com。

通讯作者:苏尚国,男,1965年生,教授,博士生导师,主要从事岩浆作用与岩浆矿床研究; E-mail: susg@cugb.edu.cn。

110034, Liaoning, China; 4. China Aero Geophysical Survey & Remote-Sensing Center for Land Resources, Beijing 100083, China; 5. Development and Research Center, China Geological Survey, Beijing 100037, China)

Abstract: Hongshan syenite complex has fairly abundant clinopyroxene with core–rim (core–mantle–rim) structure. By studying the changes in the composition of clinopyroxene, information on the genesis and evolution of rocks can be obtained. Based on detailed field geological survey, the authors used zircon U–Pb chronology and mineralogical studies to obtain the biotite pyroxene syenite zircon U–Pb dating data of Hongshan syenite complex, with the age being (126.9 ± 1.2) Ma, suggesting a product of the thinning peak period of the North China Craton lithosphere. The Mg[#] values of clinopyroxene from pyroxene syenite and biotite pyroxene syenite in the Hongshan syenite complex are 39.4–72.5 and 55.4–81.7, with characteristics of high FeO, Na₂O and CaO content and low Al₂O₃, MgO and TiO₂ content. The clinopyroxene generally had the evolutionary trend of diopside and aegirine, and reached an equilibrium state with the melt. The clinopyroxene had a Fe²⁺ to Mg²⁺ substitution relationship during the initial evolution. With the evolution, the magma became richer in sodium and iron, which suggests that the magma system had the characteristics of high temperature, medium oxygen fugacity and richness in alkali. Combined with the clinopyroxene core–rim (core–mantle–rim), the authors hold that there existed a clear contact relationship and discontinuous chemical composition. It is shown that, after the formation of the Hongshan syenite complex, it also underwent the transformation of sodium-rich and iron-rich fluids, causing the clinopyroxene to form a sodium-rich and iron-rich rim. The fluid may have modified the complex from west to east or from the inside of the Hongshan syenite complex to the outside.

Key words: syenite complex; clinopyroxene; mineralogy; zircon U–Pb chronology; Mesozoic; magma evolution; sodium-rich fluid; geological survey engineering; Wu'an; Hebei Province

About the first author: ZHANG Bo, male, born in 1986, doctor candidate, professional direction mineralogy, petrology, depositology; E-mail: zbotdw@163.com.

About the corresponding author: SU Shangguo, male, born in 1965, professor, supervisor of doctor candidates, mainly engages in the study of magmatism and magmatic deposits; E-mail: susg@cugb.edu.cn.

Funds support: Supported by National Natural Science Foundation of China (No.41272105, No.41802201), China Geology Survey Project (No. 12120115069701, No. DD20190429), Ministry of Education Doctoral Program Fund (No.20130022140001) and Natural Science Foundation of Shandong Province (No. ZR2018BD012).

1 引言

位于华北克拉通中部带的邯郸地区发育大量的中生代基性—中酸性杂岩体，并盛产铁矿，前人在该地区作了大量的基础性研究和地质调查工作，并取得了丰硕的成果(罗照华等, 1999; 许文良等, 2006, 2009; Chen et al., 2008; Deng et al., 2015; 苏尚国等, 2017)，其中东部的洪山正长岩杂岩体仅发育规模较小的铜金矿化(李随民等, 2020)，总体研究程度相对较低。岩浆岩中造岩矿物的化学组成与岩浆的物质成分、矿物的结晶环境密切相关，这些特征的变化可以在矿物成分上直接表现出来，因此可以利用矿物成分的变化特征来深入探讨岩石成因及演化机制(Dobosi and Fodor, 1992; Yang et al., 1999; 白志民, 2000; Marks et al., 2004; Gao et al., 2004, 2008; 蒋少涌等, 2006, 2008; 黄小龙等, 2007;

牛晓露等, 2009; 邹金汐等, 2012; 杨照耀等, 2015; 刘鑫和汤艳杰, 2018)。鉴于此，本文在对邯郸地区东部洪山正长岩杂岩体进行详细野外地质调查的基础上，选择富含单斜辉石矿物的辉石正长岩和黑云辉石正长岩，运用详细的矿物学手段来研究岩石的性质和岩浆演化过程。

2 地质背景和岩体地质

本文研究区位于华北克拉通中部带(图1a)，区内出露地层主要为分布于西部的前寒武纪变质地层，向东逐渐过渡到白垩纪火山岩地层，缺失志留纪、泥盆纪、侏罗纪地层；岩体由西向东依次为符山角闪闪长岩杂岩体、武安二长岩杂岩体、洪山正长岩杂岩体(图1b)。洪山正长岩杂岩体呈半圆形岩株状出露于永年区洪山沟一带的下二叠统一上三叠统，西侧部分受紫山—鼓山断裂切割下降后被第四

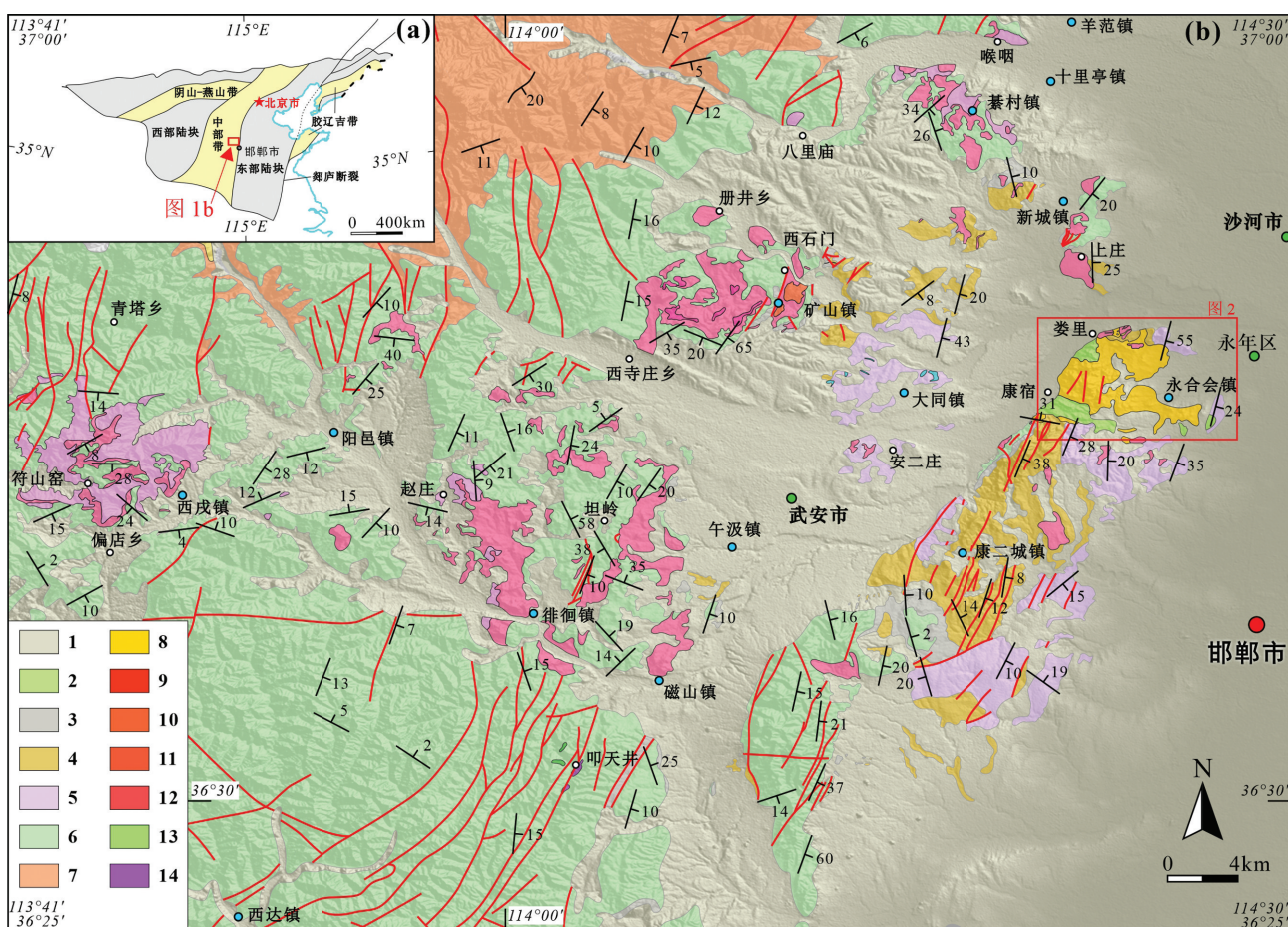


图1 华北克拉通基底构造单元划分图(a, 据 Zhao et al., 2005)和邯郸地区区域地质图(b, 据资料^{①②}修编)
 1—第四系;2—白垩纪火山岩地层;3—三叠纪沉积地层;4—二叠纪沉积地层;5—石炭纪沉积地层;6—奥陶纪沉积地层;7—前寒武变质地层;
 8—正长岩;9—二长岩;10—二长闪长岩;11—闪长岩;12—角闪闪长岩;13—橄榄辉长岩;14—辉橄岩

Fig.1 Tectonic subdivision of the North China Craton (a, after Zhao et al., 2005) and geological map of the Handan-Xintai area
 (b, modified from Zhao et al., 2008^①; Zhang et al., 2014^②)

1—Quaternary; 2—Cretaceous volcanic strata; 3—Triassic sedimentary strata; 4—Permian sedimentary strata; 5—Carboniferous sedimentary strata;
 6—Ordovician sedimentary strata; 7—Precambrian metamorphic strata; 8—Syenite; 9—Monzonite; 10—Monzodiorite; 11—Diorite; 12—Hornblende
 diorite; 13—Olivine gabbro; 14—Pyroxene peridotite

系覆盖不可见,出露面积约53 km²(张波等, 2020),杂岩体的主体是由边缘相的黑云辉石正长岩、过渡相的辉石正长岩,逐渐过渡到中心相的正长岩(图2),边缘相向中心相表现为黑云母和辉石含量逐渐降低,矿物颗粒逐渐增大,杂岩体零星分布粗面岩、辉长岩、闪长玢岩,和广泛分布的正长斑岩脉、石英脉等(图1b, 图2)。洪山正长岩杂岩体发育大量的断层(图2)。本文研究对象为过渡相靠近中心相的辉石正长岩(HS8-33)和边缘相靠近过渡相的黑云辉石正长岩(HS8-48),采样位置见图2。

辉石正长岩为浅肉红色,粗粒半自形粒状结构,块状构造,主要由钾长石(70%)、辉石(10%)、斜长石(10%)、磷灰石(5%)、磁铁矿(3%)组成,含有少

量榍石、锆石等,钾长石多为条纹长石,宽板状,发育卡式双晶,粒径约为3 mm×5 mm,发育钠长石增生边;辉石为单斜辉石,他形一半自形粒状,与磷灰石和磁铁矿共生,位于长石晶体间隙,粒径1 mm左右,部分辉石呈捕虏晶形式位于钾长石内,他形,粒径多小于0.2 mm;磷灰石呈自形一半自形粒状,与辉石共生,粒径0.3~1.0 mm;磁铁矿为立方体,位于辉石矿物颗粒间,粒径小于0.1 mm(图3a,b)。

黑云辉石正长岩为浅肉红色,中粗粒半自形粒状结构,块状构造,主要由钾长石(65%)、斜长石(15%)、辉石(10%)、黑云母(5%)、磷灰石(5%)组成,含有少量榍石、磁铁矿、锆石等,钾长石多为条纹长石,宽板状,发育卡式双晶,粒径1 mm×3 mm~3

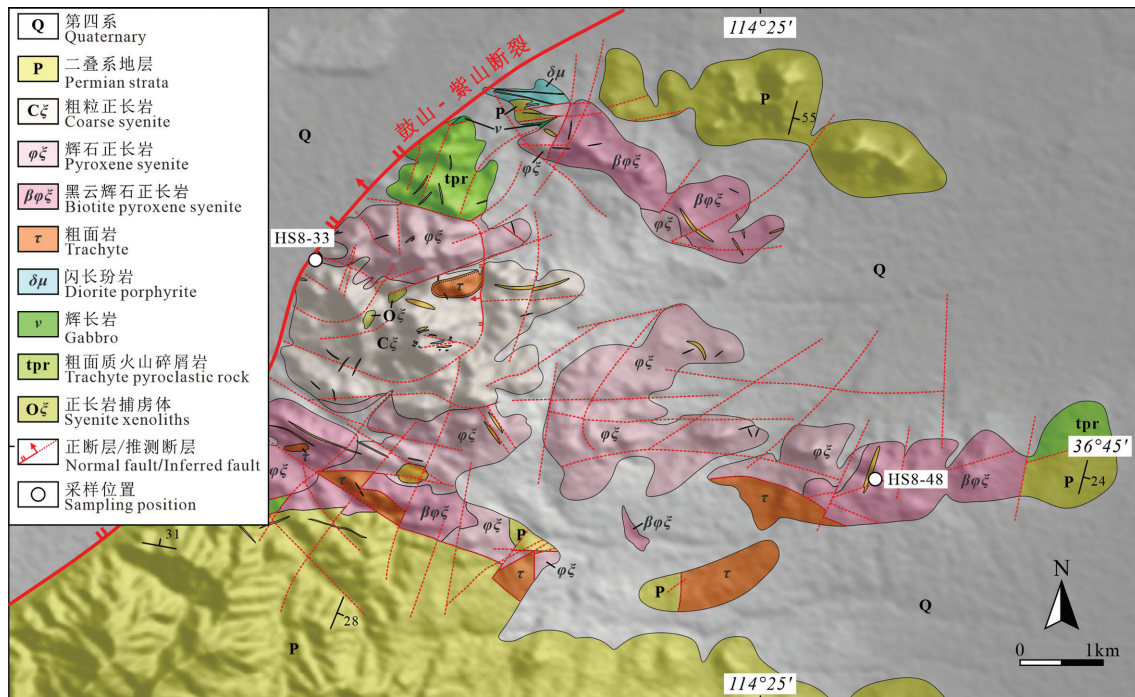


图2 洪山正长岩杂岩体地质略图

Fig.2 Geological sketch map of the Hongshan syenite complex

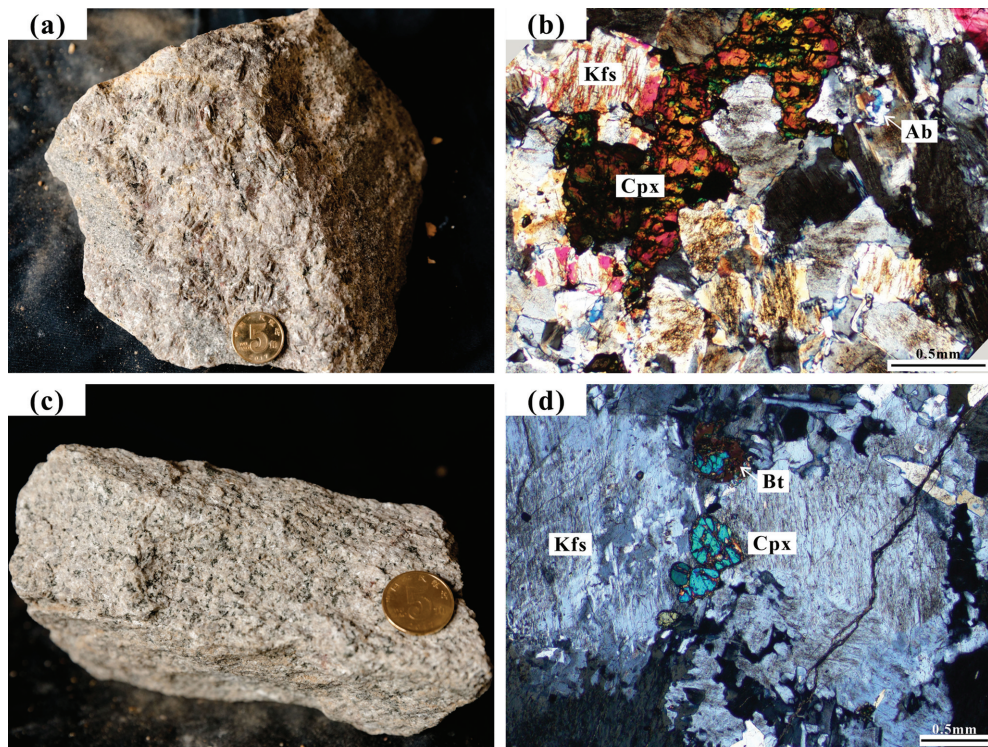


图3 洪山正长岩杂岩样品照片和镜下照片

a, b—辉石正长岩(HS8-33); c, d—黑云辉石正长岩(HS8-48). Cpx—单斜辉石; Kfs—钾长石; Ab—钠长石; Bt—黑云母

Fig.3 Sample photos and microphotograph of the Hongshan syenite complex

a, b—Pyroxene syenite (HS8-33); c, d—Biotite pyroxene syenite (HS8-48). Cpx—Clinopyroxene; Kfs—K-feldspar; Bt—Biotite

mm×5 mm; 斜长石他形—半自形粒状, 发育聚片双晶, 粒径0.5~1 mm, 常被钾长石包裹; 辉石为单斜辉石, 他形—半自形粒状, 与磷灰石和磁铁矿共生, 位于钾长石晶体间隙, 粒径1 mm左右, 部分辉石呈早期捕虏晶形式位于钾长石内, 他形, 粒径多小于0.2 mm; 黑云母片状, 粒径2~3 mm, 与辉石、磁铁矿等矿物共生; 磷灰石自形—半自形粒状, 与辉石共生, 粒径0.3~1.0 mm; 磁铁矿为立方体, 位于辉石矿物颗粒间, 粒径小于0.1 mm(图3c,d)。

3 分析方法

锆石分选及CL图像的采集在河北省区域地质矿产调查研究所实验室完成。首先将新鲜无蚀变的样品粉碎至80~100目, 并用重液和磁选方法进行分离, 最后在双目镜下提纯。将分选出的锆石颗粒黏在双面胶上, 套上靶环, 灌入环氧树脂后冷却, 对样品靶抛光露出锆石颗粒表面, 再对锆石进行透射光、反射光和阴极发光(CL)图像的采集。锆石LA-ICP-MS U-Pb年龄分析在北京锆年领航科技有限公司完成。将193 nm的ArF准分子激光与Elan 6100DRC型ICP-MS仪器连接, 采用He作为

剥蚀物质的载气, 用美国国家标准技术研究院研制的人工合成硅酸盐玻璃标准参考物质NIST 610进行仪器最佳化, Si为内标元素, 采用PLE锆石为标样进行U-Pb同位素的标定, 91500标准锆石为监控盲样。本次实验所采用的激光束斑直径为30 μm, 剥蚀频率为5 Hz, 激光能量密度为20 J/cm², 普通铅校正采用Anderson(2002)的方法, 其年龄采用Ludwig(2003)的Isoplot/Ex_ver 3.0程序计算。详细实验测试过程可参见文献Yuan et al.(2004)。矿物的主量元素分析在河北省区域地质矿产调查研究所实验室的电子探针上完成, 分析仪器型号为JXA-8230, 加速电压15 kV, 束流1×10⁻⁸A, 束斑1~10 μm。采用PRZ方法校正, 分析标样为美国SPI公司的53种矿物, 测试精度优于1%。

4 分析结果

4.1 锆石U-Pb年代学

本文在洪山正长岩杂岩体中黑云辉石正长岩采集1件样品进行锆石U-Pb年代学工作, 采样位置为: 36°44'45.8"N、114°25'52.8"E。本文锆石U-Pb测年样品代表性锆石CL图像见图4a, U-Pb分析结

表1 洪山正长岩杂岩体锆石LA-ICP-MS U-Pb年龄数据
Table 1 LA-ICP-MS U-Pb zircon ages of Hongshan syenite complex

| 测点号 | 含量/ 10^{-6} | | | | 同位素比值 | | | | 年龄/Ma | | | |
|------------------------|---------------|--------|-------|------|-----------------------------------|----------------------------------|----------------------------------|-----------------------------------|----------------------------------|----------------------------------|----------------------------------|----------------------------------|
| | Pb | Th | U | Th/U | $^{207}\text{Pb}/^{206}\text{Pb}$ | $^{207}\text{Pb}/^{235}\text{U}$ | $^{206}\text{Pb}/^{238}\text{U}$ | $^{207}\text{Pb}/^{206}\text{Pb}$ | $^{207}\text{Pb}/^{235}\text{U}$ | $^{206}\text{Pb}/^{238}\text{U}$ | $^{207}\text{Pb}/^{235}\text{U}$ | $^{206}\text{Pb}/^{238}\text{U}$ |
| 黑云辉石正长岩(HS8-48) | | | | | | | | | | | | |
| 1 | 17.9 | 140.9 | 148.1 | 0.95 | 0.0493±22 | 0.1307±57 | 0.0194±4 | 161.2±103.7 | 124.7±5.1 | 123.9±2.4 | | |
| 2 | 138.4 | 1443.1 | 775.2 | 1.86 | 0.0494±12 | 0.1193±53 | 0.0174±5 | 168.6±62.0 | 114.4±4.8 | 111.2±2.9 | | |
| 3 | 15.1 | 111.3 | 143.7 | 0.77 | 0.0532±25 | 0.1416±67 | 0.0195±5 | 344.5±105.5 | 134.4±6.0 | 124.4±3.1 | | |
| 4 | 49.8 | 395.4 | 326.9 | 1.21 | 0.0476±14 | 0.1304±38 | 0.0200±3 | 79.7±72.2 | 124.5±3.4 | 127.6±2.1 | | |
| 5 | 42.1 | 355.2 | 326.2 | 1.09 | 0.0552±24 | 0.1366±55 | 0.0181±4 | 420.4±100.9 | 130.0±5.0 | 115.4±2.8 | | |
| 6 | 13.8 | 115.4 | 144.0 | 0.80 | 0.0525±26 | 0.1370±74 | 0.0190±4 | 305.6±114.8 | 130.3±6.6 | 121.2±2.4 | | |
| 7 | 24.2 | 165.5 | 181.8 | 0.91 | 0.1007±52 | 0.2457±137 | 0.0177±4 | 1638.9±96.3 | 223.1±11.2 | 113.1±2.2 | | |
| 8 | 22.4 | 180.2 | 191.6 | 0.94 | 0.0484±22 | 0.1331±64 | 0.0201±4 | 120.5±112.0 | 126.9±5.8 | 128.3±2.8 | | |
| 9 | 45.1 | 246.0 | 242.3 | 1.02 | 0.1302±56 | 0.3312±137 | 0.0185±4 | 2101.9±71.3 | 290.5±10.5 | 118.1±2.3 | | |
| 10 | 33.7 | 259.7 | 222.4 | 1.17 | 0.0472±16 | 0.1285±46 | 0.0199±4 | 61.2±138.9 | 122.8±4.1 | 126.9±2.6 | | |
| 11 | 14.9 | 110.1 | 154.0 | 0.71 | 0.0509±23 | 0.1377±64 | 0.0198±4 | 235.3±105.5 | 131.0±5.7 | 126.5±2.6 | | |
| 12 | 19.0 | 171.6 | 194.0 | 0.88 | 0.0560±26 | 0.1398±70 | 0.0181±3 | 453.8±103.7 | 132.8±6.2 | 115.6±2.0 | | |
| 13 | 15.7 | 144.1 | 167.3 | 0.86 | 0.0501±22 | 0.1339±62 | 0.0195±3 | 211.2±100.0 | 127.6±5.5 | 124.2±2.2 | | |
| 14 | 65.2 | 597.4 | 640.7 | 0.93 | 0.0533±10 | 0.1188±25 | 0.0162±2 | 338.9±42.6 | 114.0±2.3 | 103.4±1.3 | | |
| 15 | 37.4 | 314.5 | 303.6 | 1.04 | 0.0603±32 | 0.1421±76 | 0.0171±3 | 616.7±113.7 | 134.9±6.8 | 109.5±2.2 | | |
| 16 | 16.9 | 125.8 | 152.5 | 0.83 | 0.0535±21 | 0.1461±55 | 0.0199±4 | 350.1±87.0 | 138.5±4.9 | 127.0±2.3 | | |
| 17 | 21.3 | 175.9 | 195.0 | 0.90 | 0.0490±24 | 0.1311±63 | 0.0196±4 | 150.1±116.7 | 125.1±5.7 | 125.4±2.3 | | |
| 18 | 14.7 | 102.2 | 142.0 | 0.72 | 0.0531±30 | 0.1429±73 | 0.0199±4 | 344.5±129.6 | 135.6±6.5 | 126.7±2.6 | | |
| 19 | 25.5 | 162.4 | 172.7 | 0.94 | 0.0533±20 | 0.1527±66 | 0.0207±3 | 342.7±89.8 | 144.3±5.8 | 132.3±2.1 | | |
| 20 | 43.7 | 333.9 | 329.3 | 1.01 | 0.0503±13 | 0.1342±38 | 0.0194±4 | 209.3±91.7 | 127.9±3.4 | 123.9±2.2 | | |
| 21 | 29.2 | 234.0 | 232.8 | 1.01 | 0.0521±14 | 0.1440±48 | 0.0201±4 | 300.1±63.0 | 136.6±4.3 | 128.0±2.8 | | |
| 22 | 18.1 | 157.9 | 176.0 | 0.90 | 0.0447±20 | 0.1212±52 | 0.0199±4 | / | 116.2±4.7 | 127.3±2.6 | | |
| 23 | 29.8 | 215.5 | 249.8 | 0.86 | 0.0557±24 | 0.1700±86 | 0.0220±5 | 438.9±130.5 | 159.4±7.5 | 140.5±3.1 | | |
| 24 | 36.2 | 281.7 | 285.2 | 0.99 | 0.0784±46 | 0.1984±106 | 0.0186±8 | 1166.7±121.3 | 183.8±9.0 | 119.0±5.0 | | |
| 25 | 10.8 | 71.2 | 129.6 | 0.55 | 0.0476±23 | 0.1338±68 | 0.0205±4 | 79.7±111.1 | 127.5±6.1 | 130.7±2.7 | | |

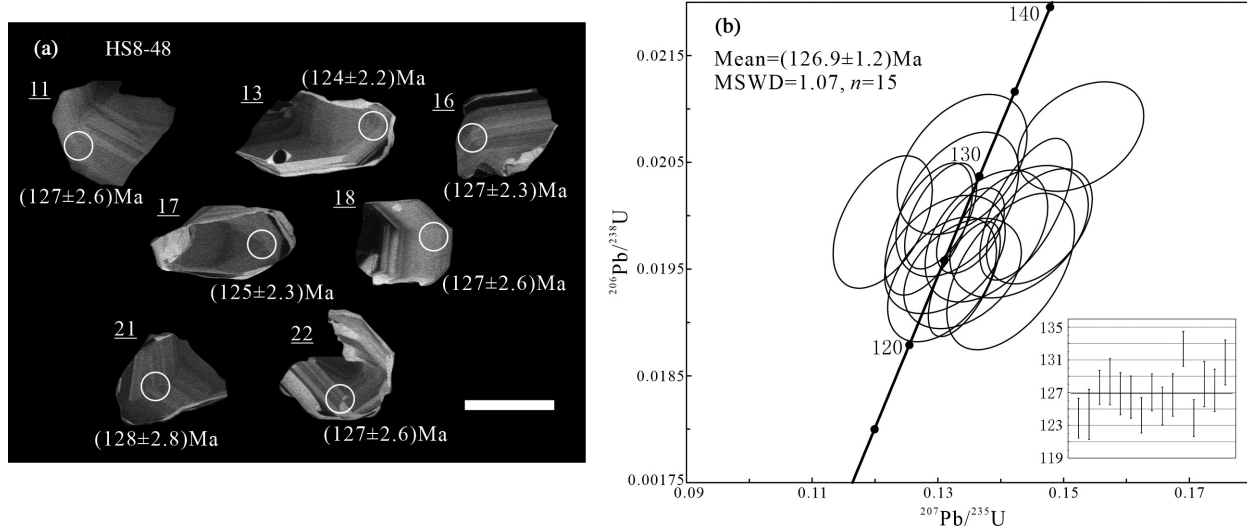


图4 洪山正长岩杂岩体代表性锆石的CL图像(a)和锆石U-Pb年龄谐和曲线(b)

Fig.4 Representative cathodoluminescence (CL) images of zircon grains (a) and U-Pb concordia diagrams of zircons (b) from the Hongshan syenite complex

果见表1。

从CL图像中可以看出,锆石基本均呈自形晶,内部结构清晰,多数锆石振荡生长环带发育。具有相对较高的Th/U比值(0.55~1.86),暗示它们为岩浆成因。黑云辉石正长岩(HS8-48)中25颗锆石进行了25个点的测试分析,除其中10个测点数据较离散外,其余15个测点的 $^{206}\text{Pb}/^{238}\text{U}$ 年龄介于123.9~132.3 Ma,在 $^{206}\text{Pb}/^{238}\text{U}$ - $^{207}\text{Pb}/^{235}\text{U}$ 谐和线上或其附近(图4b), $^{206}\text{Pb}/^{238}\text{U}$ 年龄加权平均值为(126.9±1.2)Ma(1σ ,MSWD=1.07,n=15)。

4.2 辉石成分特征及分类

在背散射(BSE)图像中,可以清楚地发现单斜辉石(Cpx)具有复杂的结构特征,辉石正长岩(HS8-33)中Cpx多发育核-边结构,表现为核部形状不规则、颜色较深,被颜色较浅、宽度较窄的边部包裹(图5a,b),核-边界线截然,以溶蚀的港湾状为主,以不发育明显环带为特征;而黑云辉石正长岩(HS8-48)中Cpx有的发育与辉石正长岩中Cpx类似的核-边结构,有的发育核-幔-边结构,核部发育形状不规则、颜色较浅的斑块区(Goleñ, 2015),幔部为颜色较深的主体Cpx,边部则发育颜色较浅的外带(图5c,d),核-幔-边界线同样截然,以溶蚀的港湾状为主,同样以不发育明显环带为特征。电子探针数据(表2)表明,辉石正长岩和黑云辉石正长岩中Cpx的Mg[#]值分别在39.4~72.5、55.4~81.7,除一个Mg[#]值较

高的点(图5d, 4-10点)外,其SiO₂含量分别为51.00%~53.75%、50.89%~52.82%;Al₂O₃含量分别为0.28%~2.98%、0.99%~2.40%;MgO含量分别为6.67%~12.93%、9.35%~13.16%;FeO*含量分别为8.74%~18.27%、8.30%~13.45%;CaO含量分别为17.74%~23.10%、21.22%~23.22%;Na₂O含量分别为0.91%~3.75%、0.80%~1.77%;TiO₂含量分别为0.10%~0.55%、0.12%~0.61%。总的来说,辉石正长岩和黑云辉石正长岩中Cpx均具有较高的FeO、Na₂O、CaO含量,较低Al₂O₃、MgO、TiO₂含量的特征,黑云辉石正长岩中Cpx主量元素的变化范围更小,辉石正长岩中Cpx核部和黑云辉石正长岩中Cpx幔部均具有较高的SiO₂、TiO₂、Al₂O₃、MgO、CaO含量和Mg[#]值。黑云辉石正长岩中Cpx而核部和边部具有几乎一致的主量元素含量特征(表2,图7),通过仔细观察和对比,这种现象的产生很可能是由于边部Cpx呈枝状嵌入幔部Cpx,后来在样品加工过程中切割矿物造成的“捕虏晶”假象。

依据Morimoto(1988)提出的辉石分类命名方案,本文中的黑云辉石正长岩中Cpx均位于Q-J图解($Q=\text{Ca}+\text{Mg}+\text{Fe}^{2+}$, $J=2\text{Na}^+$)的Ca-Mg-Fe区域内,且位置较为集中,而辉石正长岩中Cpx则横跨了Ca-Mg-Fe和Ca-Na区域,并表现为不连续的分组特征(图6a),主要表现为核部Cpx主要位于Ca-Mg-Fe区域,而边部Cpx主要位于Ca-Na区域;将

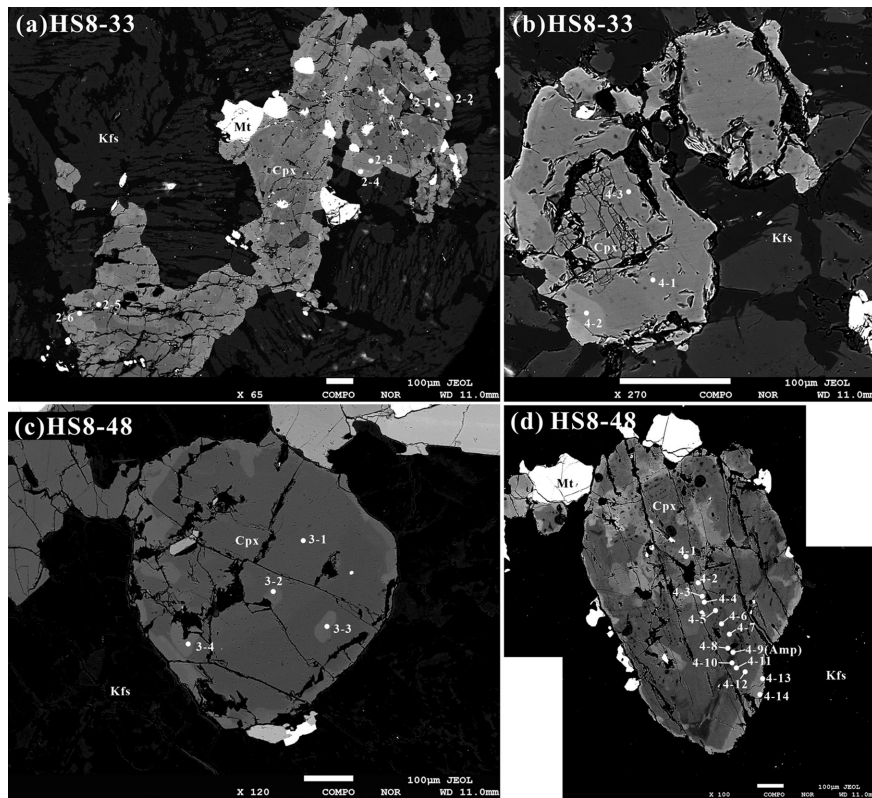
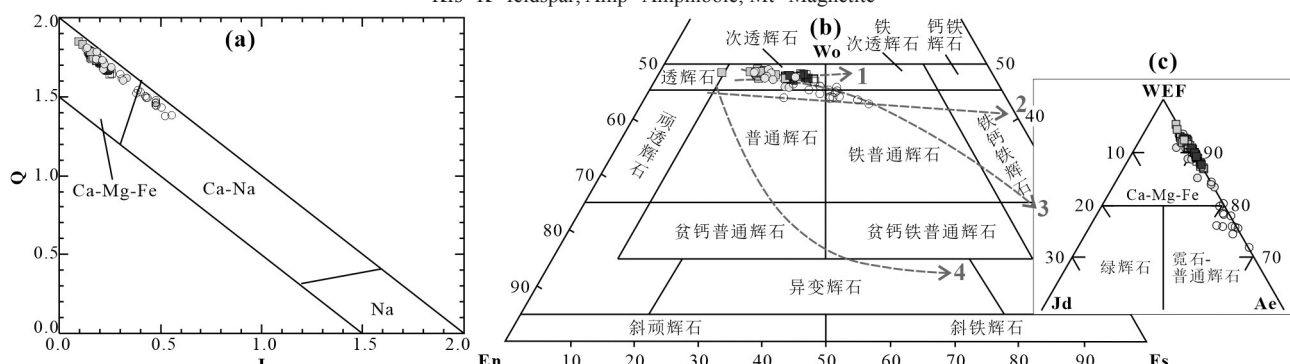


图5 洪山正长岩杂岩体中代表性单斜辉石的BSE图像

a, b—辉石正长岩(HS8-33); c, d—黑云辉石正长岩(HS8-48); Cpx—单斜辉石; Kfs—钾长石; Mt—磁铁矿

Fig. 5 Representative BSE images of the of clinopyroxene from the Hongshan syenite complex

a, b—Pyroxene syenite (HS8-33); c, d—Biotite pyroxene syenite (HS8-48); Cpx—clinopyroxene;
Kfs—K-feldspar; Amp—Amphibole; Mt—Magnetite



○辉石正长岩辉石核部 □辉石正长岩辉石边部 ■黑云辉石正长岩辉石核部 ▨黑云辉石正长岩辉石幔部 ▨黑云辉石正长岩辉石边部
Pyroxene syenite(core) Pyroxene syenite(rim) Biotite pyroxene syenite(core) Biotite pyroxene syenite(mantle) Biotite pyroxene syenite(rim)

图6 洪山正长岩杂岩体单斜辉石系列划分图解(a)和单斜辉石分类图解(b、c)(据 Morimoto, 1988; 邱家骥和廖群安, 1996 修改)

Wo—硅灰石; En—斜顽辉石; Fs—斜铁辉石; WEF—Wo—En—Fs 端元; Jd—硬玉; Ae—霓石; 图b中演化趋势分别为:

1—钙铁辉石→透辉石 (Baie-des-Moutons 正长岩质杂岩体早期正长岩中, Lalonde and Marin, 1983); 2—透辉石→钙铁辉石 (日本碱性玄武岩系列, Aoki, 1964;

Shiant Isles 岩体, Gibb, 1972); 3—透辉石→霓石 (Shonkin Sag 岩体, Nash and Wilkinson, 1970); 4—透辉石→易变辉石 (日本拉斑质玄武岩, Kuno, 1955)

Fig. 6 Discrimination diagram of the series for pyroxene (a) and discrimination diagram of clinopyroxene (b, c) from the Hongshan syenite complex (modified from Morimoto, 1988; Qiu Jiaxiang and Liao Qun'an, 1996)

Wo—Wollastonite; En—Clinoenstatite; Fs—Clinoferro; WEF—Wo—En—Fs end member; Jd—Jadeite; Ae—Aegirine;

Fig. b shown for comparison exhibiting crystallization trends of other different types of magmas; 1—Hedenbergite → diopside (Baie-des-Moutons syenitic complex, early-group syenites. After Lalonde and Marin, 1983); 2—Diopside → hedenbergite (Japanese alkaline basalt series, after Aoki, 1964; Shiant Isles sill, Gibb, 1972); 3—Diopside → aegirine (Shonkin Sag laccolith, after Nash and Wilkinson, 1970); 4—Diopside → ferropigeonite (Japanese tholeiite series, after Kuno, 1955)

表2 洪山正长岩杂岩体中单斜辉石电子探针数据(%)

| 岩石类型 点号 | 辉石正长岩(HS8-33) | | | | | | | | | | 辉石正长岩(HS8-33) | | | | | | | | | | | | | | |
|--------------------------------|---------------|-------|--------|-------|-------|--------|-------|-------|--------|-------|---------------|--------|-------|-------|-------|-------|-------|--------|-------|-------|-------|--------|--------|-------|-------|
| | 2-1 | 2-2 | 2-3 | 2-4 | 2-5 | 2-6 | 4-1 | 4-2 | 4-3 | 5-1 | 5-2 | 6-1 | 6-2 | 6-3 | 6-4 | 6-5 | 6-6 | 6-7 | 6-8 | 6-9 | 8-1 | 8-2 | 8-3 | | |
| SiO ₂ | 51.00 | 51.17 | 52.04 | 51.70 | 53.32 | 52.47 | 52.28 | 52.02 | 52.44 | 51.01 | 52.07 | 52.58 | 52.12 | 53.17 | 51.73 | 51.65 | 51.38 | 51.63 | 53.75 | 51.23 | 51.74 | 51.56 | 51.74 | 52.87 | 51.10 |
| TiO ₂ | 0.55 | 0.29 | 0.26 | 0.32 | 0.19 | 0.28 | 0.45 | 0.24 | 0.37 | 0.23 | 0.46 | 0.11 | 0.21 | 0.10 | 0.26 | 0.14 | 0.20 | 0.23 | 0.21 | 0.35 | 0.50 | 0.25 | 0.47 | 0.15 | 0.22 |
| Al ₂ O ₃ | 2.98 | 1.34 | 1.08 | 1.38 | 0.73 | 1.32 | 1.46 | 1.19 | 1.35 | 1.35 | 1.75 | 0.28 | 0.86 | 0.46 | 1.30 | 1.15 | 0.68 | 1.23 | 0.46 | 1.29 | 1.92 | 1.50 | 1.80 | 0.68 | 1.45 |
| FeO* | 9.79 | 15.43 | 13.49 | 15.13 | 9.67 | 15.23 | 8.75 | 12.13 | 8.74 | 15.29 | 9.94 | 11.45 | 14.28 | 11.78 | 15.27 | 13.84 | 18.27 | 15.59 | 11.76 | 15.18 | 9.64 | 11.96 | 9.53 | 10.42 | 14.66 |
| Cr ₂ O ₃ | 0.01 | 0.00 | 0.07 | 0.05 | 0.02 | 0.00 | 0.02 | 0.01 | 0.00 | 0.00 | 0.01 | 0.01 | 0.04 | 0.00 | 0.03 | 0.00 | 0.02 | 0.01 | 0.01 | 0.00 | 0.03 | 0.01 | 0.01 | 0.00 | 0.00 |
| MnO | 0.48 | 0.98 | 0.88 | 0.94 | 0.63 | 0.91 | 0.52 | 0.90 | 0.50 | 0.88 | 0.63 | 1.14 | 1.05 | 1.01 | 0.79 | 1.06 | 0.96 | 0.97 | 1.05 | 0.89 | 0.61 | 0.75 | 0.72 | 0.86 | 0.95 |
| MgO | 11.87 | 8.03 | 9.69 | 8.14 | 12.16 | 8.30 | 12.93 | 10.61 | 12.67 | 8.11 | 11.62 | 11.30 | 9.13 | 10.92 | 8.53 | 8.87 | 6.67 | 7.92 | 11.46 | 8.58 | 12.21 | 10.19 | 11.80 | 11.91 | 8.44 |
| CaO | 21.85 | 19.23 | 19.93 | 18.51 | 21.92 | 18.49 | 23.10 | 21.02 | 22.92 | 18.98 | 22.24 | 21.10 | 19.38 | 20.71 | 18.78 | 19.89 | 17.74 | 18.43 | 19.83 | 18.58 | 22.01 | 21.32 | 22.82 | 22.07 | 19.34 |
| Na ₂ O | 1.52 | 2.89 | 2.68 | 3.25 | 1.28 | 3.27 | 0.91 | 2.13 | 0.95 | 3.22 | 1.56 | 1.77 | 3.00 | 2.31 | 3.25 | 2.73 | 3.75 | 3.43 | 2.09 | 3.26 | 1.27 | 2.17 | 1.26 | 1.48 | 2.91 |
| K ₂ O | 0.01 | 0.00 | 0.01 | 0.00 | 0.00 | 0.00 | 0.01 | 0.01 | 0.02 | 0.01 | 0.00 | 0.00 | 0.03 | 0.00 | 0.00 | 0.01 | 0.00 | 0.01 | 0.03 | 0.02 | 0.00 | 0.00 | 0.00 | 0.00 | |
| Total | 100.05 | 99.34 | 100.12 | 99.41 | 99.91 | 100.26 | 99.03 | 99.08 | 100.26 | 99.74 | 100.08 | 100.50 | 99.90 | 99.90 | 99.36 | 99.65 | 99.45 | 100.65 | 99.40 | 99.89 | 99.74 | 100.15 | 100.44 | 99.07 | |
| 阳离子数(以6个氧原子计算) | | | | | | | | | | | | | | | | | | | | | | | | | |
| TSi | 1.90 | 1.95 | 1.95 | 1.96 | 1.99 | 1.98 | 1.94 | 1.95 | 1.94 | 1.94 | 1.98 | 1.96 | 1.96 | 1.98 | 1.95 | 1.96 | 1.96 | 1.96 | 1.96 | 1.94 | 1.93 | 1.94 | 1.93 | 1.97 | 1.95 |
| TAI | 0.10 | 0.05 | 0.04 | 0.01 | 0.03 | 0.06 | 0.05 | 0.05 | 0.06 | 0.06 | 0.01 | 0.04 | 0.02 | 0.05 | 0.04 | 0.03 | 0.04 | 0.03 | 0.04 | 0.00 | 0.06 | 0.07 | 0.06 | 0.07 | 0.05 |
| T Fe ³⁺ | 0.00 | 0.00 | 0.00 | 0.00 | 0.00 | 0.00 | 0.00 | 0.00 | 0.00 | 0.00 | 0.01 | 0.00 | 0.00 | 0.00 | 0.00 | 0.01 | 0.00 | 0.01 | 0.00 | 0.00 | 0.00 | 0.00 | 0.00 | 0.00 | |
| M1 Al | 0.03 | 0.01 | 0.00 | 0.03 | 0.02 | 0.03 | 0.00 | 0.01 | 0.01 | 0.01 | 0.01 | 0.00 | 0.00 | 0.00 | 0.01 | 0.01 | 0.01 | 0.01 | 0.01 | 0.02 | 0.00 | 0.02 | 0.00 | 0.01 | |
| M1 Ti | 0.02 | 0.01 | 0.01 | 0.01 | 0.01 | 0.01 | 0.01 | 0.01 | 0.01 | 0.01 | 0.01 | 0.01 | 0.01 | 0.01 | 0.01 | 0.01 | 0.01 | 0.01 | 0.01 | 0.01 | 0.01 | 0.01 | 0.01 | 0.01 | |
| M1 Fe ³⁺ | 0.16 | 0.23 | 0.23 | 0.23 | 0.07 | 0.21 | 0.10 | 0.20 | 0.08 | 0.28 | 0.13 | 0.15 | 0.25 | 0.18 | 0.26 | 0.22 | 0.30 | 0.26 | 0.12 | 0.28 | 0.12 | 0.20 | 0.13 | 0.24 | |
| M1 Fe ²⁺ | 0.14 | 0.26 | 0.20 | 0.25 | 0.23 | 0.27 | 0.17 | 0.18 | 0.19 | 0.21 | 0.18 | 0.20 | 0.20 | 0.19 | 0.22 | 0.22 | 0.28 | 0.23 | 0.22 | 0.20 | 0.17 | 0.17 | 0.17 | 0.22 | |
| M1 Cr | 0.00 | 0.00 | 0.00 | 0.00 | 0.00 | 0.00 | 0.00 | 0.00 | 0.00 | 0.00 | 0.00 | 0.00 | 0.00 | 0.00 | 0.00 | 0.00 | 0.00 | 0.00 | 0.00 | 0.00 | 0.00 | 0.00 | 0.00 | 0.00 | |
| M1 Mg | 0.66 | 0.46 | 0.54 | 0.46 | 0.68 | 0.47 | 0.72 | 0.59 | 0.70 | 0.46 | 0.64 | 0.63 | 0.51 | 0.61 | 0.48 | 0.50 | 0.38 | 0.45 | 0.64 | 0.49 | 0.68 | 0.57 | 0.66 | 0.68 | |
| M2 Fe ²⁺ | 0.01 | 0.00 | 0.00 | 0.00 | 0.01 | 0.00 | 0.00 | 0.00 | 0.00 | 0.00 | 0.00 | 0.00 | 0.00 | 0.00 | 0.00 | 0.00 | 0.00 | 0.00 | 0.00 | 0.01 | 0.00 | 0.00 | 0.00 | 0.00 | |
| M2 Mn | 0.02 | 0.03 | 0.03 | 0.02 | 0.03 | 0.02 | 0.03 | 0.02 | 0.03 | 0.02 | 0.04 | 0.03 | 0.03 | 0.03 | 0.03 | 0.03 | 0.03 | 0.03 | 0.03 | 0.02 | 0.02 | 0.02 | 0.03 | 0.03 | |
| M2 Ca | 0.87 | 0.79 | 0.80 | 0.75 | 0.88 | 0.75 | 0.92 | 0.84 | 0.92 | 0.78 | 0.89 | 0.85 | 0.78 | 0.83 | 0.76 | 0.81 | 0.73 | 0.75 | 0.79 | 0.76 | 0.88 | 0.86 | 0.91 | 0.88 | |
| M2 Na | 0.11 | 0.21 | 0.20 | 0.24 | 0.09 | 0.24 | 0.07 | 0.16 | 0.07 | 0.24 | 0.11 | 0.13 | 0.22 | 0.17 | 0.24 | 0.20 | 0.28 | 0.25 | 0.15 | 0.24 | 0.09 | 0.16 | 0.09 | 0.11 | |
| M2 K | 0.00 | 0.00 | 0.00 | 0.00 | 0.00 | 0.00 | 0.00 | 0.00 | 0.00 | 0.00 | 0.00 | 0.00 | 0.00 | 0.00 | 0.00 | 0.00 | 0.00 | 0.00 | 0.00 | 0.00 | 0.00 | 0.00 | 0.00 | 0.00 | |
| 计算辉石的端元组分 | | | | | | | | | | | | | | | | | | | | | | | | | |
| Wo | 47.10 | 44.50 | 44.65 | 43.68 | 46.77 | 43.35 | 47.80 | 45.75 | 47.98 | 44.25 | 47.67 | 45.22 | 43.98 | 45.12 | 43.48 | 45.34 | 42.19 | 43.48 | 43.31 | 43.13 | 46.83 | 46.94 | 48.31 | 46.50 | 44.69 |
| En | 35.62 | 25.85 | 30.21 | 26.71 | 36.08 | 27.09 | 37.23 | 32.12 | 36.91 | 26.30 | 34.65 | 33.70 | 28.84 | 33.10 | 27.48 | 28.13 | 22.08 | 26.01 | 34.83 | 27.72 | 36.14 | 31.20 | 34.75 | 34.93 | 27.13 |
| Fs | 17.29 | 29.66 | 25.14 | 29.61 | 17.15 | 29.55 | 14.98 | 22.14 | 15.11 | 29.45 | 17.69 | 21.08 | 27.18 | 21.78 | 29.05 | 26.53 | 35.73 | 30.51 | 21.86 | 29.14 | 17.03 | 21.86 | 16.95 | 18.57 | 28.18 |
| Wef | 88.56 | 78.22 | 80.10 | 75.72 | 90.69 | 75.91 | 93.27 | 84.15 | 93.01 | 75.63 | 88.48 | 87.00 | 77.75 | 83.19 | 75.74 | 79.54 | 71.76 | 74.30 | 84.95 | 75.41 | 90.52 | 83.70 | 90.61 | 89.14 | 78.01 |
| Jd | 1.69 | 1.09 | 0.06 | 2.38 | 2.53 | 3.27 | 0.10 | 0.00 | 0.92 | 0.38 | 1.12 | 0.00 | 0.00 | 0.00 | 0.81 | 0.97 | 0.00 | 1.42 | 1.93 | 0.00 | 1.07 | 0.31 | 0.55 | 0.00 | 1.06 |
| Ae | 9.76 | 20.69 | 19.84 | 21.91 | 6.78 | 20.82 | 6.63 | 15.85 | 6.07 | 23.99 | 10.40 | 13.01 | 22.25 | 16.81 | 23.45 | 19.49 | 28.24 | 24.28 | 13.13 | 24.59 | 8.41 | 15.99 | 8.84 | 10.86 | 20.93 |
| Mg [#] | 68.38 | 48.12 | 56.15 | 48.95 | 69.15 | 49.29 | 72.48 | 60.92 | 72.11 | 48.59 | 67.57 | 63.76 | 53.28 | 62.29 | 49.89 | 53.33 | 39.43 | 47.53 | 63.47 | 50.19 | 69.30 | 60.29 | 68.81 | 67.09 | 50.64 |

续表2

| 黑云辉石正长岩(HS8-48) | | | | | | | | | | | | | | | | | | | | | | | | | | |
|--------------------------------|-------|--------|-------|--------|-------|-------|--------|--------|-------|--------|--------|--------|--------|--------|--------|-------|-------|--------|--------|--------|--------|--------|--------|-------|--------|------|
| 岩石类型 | 点号 | 1-1 | 1-2 | 1-3 | 2-1 | 2-2 | 2-3 | 2-4 | 2-5 | 2-6 | 2-7 | 3-1 | 3-2 | 3-3 | 3-4 | 3-5 | 3-6 | 4-1 | 4-2 | 4-3 | 4-4 | 4-5 | 4-6 | 4-7 | 4-8 | 4-10 |
| 部位 | 核 | 幔 | 边 | 边 | 边 | 边 | 边 | 边 | 幔 | 边 | 幔 | 核 | 核 | 核 | 核 | 幔 | 边 | 幔 | 核 | 核 | 幔 | 幔 | 幔 | 幔 | 幔 | |
| SiO ₂ | 51.24 | 52.16 | 50.89 | 51.52 | 51.49 | 52.12 | 51.88 | 51.95 | 52.06 | 51.59 | 52.45 | 51.37 | 51.40 | 51.27 | 52.14 | 51.09 | 51.83 | 52.10 | 51.72 | 52.33 | 51.86 | 52.50 | 52.08 | 51.34 | 53.65 | |
| TiO ₂ | 0.20 | 0.48 | 0.25 | 0.37 | 0.12 | 0.35 | 0.31 | 0.23 | 0.33 | 0.29 | 0.35 | 0.28 | 0.35 | 0.20 | 0.40 | 0.28 | 0.33 | 0.17 | 0.27 | 0.30 | 0.49 | 0.14 | 0.32 | 0.54 | 0.21 | |
| Al ₂ O ₃ | 1.06 | 1.56 | 1.29 | 1.45 | 0.99 | 1.54 | 1.21 | 1.28 | 1.31 | 1.31 | 1.39 | 1.51 | 1.25 | 1.23 | 1.32 | 1.41 | 1.15 | 1.12 | 1.18 | 1.29 | 1.65 | 1.35 | 1.49 | 1.89 | 0.86 | |
| FeO* | 12.64 | 9.10 | 12.29 | 11.44 | 13.37 | 9.12 | 11.57 | 12.00 | 9.21 | 12.49 | 9.14 | 12.23 | 12.70 | 13.33 | 9.29 | 12.81 | 10.37 | 11.50 | 11.40 | 9.21 | 9.10 | 8.74 | 8.96 | 9.03 | 6.00 | |
| Cr ₂ O ₃ | 0.00 | 0.00 | 0.00 | 0.00 | 0.01 | 0.01 | 0.03 | 0.02 | 0.00 | 0.01 | 0.03 | 0.04 | 0.02 | 0.00 | 0.01 | 0.01 | 0.02 | 0.00 | 0.02 | 0.03 | 0.01 | 0.01 | 0.03 | 0.00 | 0.09 | |
| MnO | 1.25 | 0.58 | 0.98 | 0.76 | 1.51 | 0.63 | 0.89 | 0.94 | 0.70 | 0.96 | 0.61 | 0.87 | 1.05 | 1.02 | 0.65 | 1.01 | 0.79 | 0.85 | 0.86 | 0.65 | 0.66 | 0.60 | 0.54 | 0.56 | 0.25 | |
| MgO | 9.86 | 12.85 | 10.01 | 11.02 | 9.44 | 12.54 | 10.95 | 10.56 | 12.75 | 10.14 | 12.82 | 10.75 | 10.19 | 9.84 | 12.34 | 9.73 | 11.56 | 10.92 | 11.04 | 12.34 | 12.24 | 12.54 | 12.75 | 12.03 | 14.99 | |
| CaO | 21.60 | 22.70 | 22.02 | 22.20 | 21.22 | 22.58 | 22.34 | 22.06 | 22.38 | 21.94 | 22.87 | 21.74 | 22.49 | 21.87 | 22.97 | 21.89 | 22.33 | 22.19 | 22.22 | 22.92 | 22.89 | 23.19 | 22.78 | 22.32 | 23.54 | |
| Na ₂ O | 1.63 | 1.07 | 1.25 | 1.37 | 1.77 | 1.00 | 1.30 | 1.29 | 1.04 | 1.50 | 1.04 | 1.64 | 1.25 | 1.37 | 1.10 | 1.47 | 1.16 | 1.48 | 1.16 | 1.68 | 1.20 | 1.29 | 1.05 | 1.09 | 1.74 | 0.68 |
| K ₂ O | 0.01 | 0.00 | 0.00 | 0.03 | 0.00 | 0.00 | 0.03 | 0.00 | 0.00 | 0.02 | 0.00 | 0.02 | 0.01 | 0.00 | 0.00 | 0.00 | 0.00 | 0.00 | 0.01 | 0.01 | 0.07 | 0.05 | 0.06 | 0.18 | 0.04 | |
| Total | 99.50 | 100.49 | 98.98 | 100.15 | 99.92 | 99.88 | 100.50 | 100.32 | 99.80 | 100.25 | 100.69 | 100.43 | 100.71 | 100.13 | 100.21 | 99.70 | 99.55 | 100.32 | 100.40 | 100.27 | 100.25 | 100.17 | 100.09 | 99.63 | 100.29 | |
| 阳离子数(以6个氧原子计算) | | | | | | | | | | | | | | | | | | | | | | | | | | |
| T Si | 1.95 | 1.93 | 1.95 | 1.93 | 1.95 | 1.95 | 1.94 | 1.95 | 1.94 | 1.94 | 1.94 | 1.92 | 1.93 | 1.94 | 1.94 | 1.94 | 1.95 | 1.95 | 1.93 | 1.95 | 1.93 | 1.95 | 1.94 | 1.91 | 1.97 | |
| T Al | 0.05 | 0.07 | 0.06 | 0.06 | 0.04 | 0.06 | 0.05 | 0.05 | 0.06 | 0.06 | 0.06 | 0.07 | 0.06 | 0.06 | 0.06 | 0.05 | 0.05 | 0.05 | 0.05 | 0.06 | 0.05 | 0.07 | 0.05 | 0.08 | 0.03 | |
| T Fe ³⁺ | 0.01 | 0.00 | 0.00 | 0.00 | 0.00 | 0.00 | 0.00 | 0.00 | 0.00 | 0.00 | 0.00 | 0.00 | 0.01 | 0.00 | 0.00 | 0.00 | 0.00 | 0.00 | 0.02 | 0.00 | 0.00 | 0.00 | 0.00 | 0.01 | 0.00 | |
| M1 Al | 0.00 | 0.00 | 0.00 | 0.00 | 0.00 | 0.01 | 0.00 | 0.01 | 0.00 | 0.00 | 0.00 | 0.00 | 0.00 | 0.00 | 0.00 | 0.00 | 0.00 | 0.00 | 0.00 | 0.00 | 0.00 | 0.00 | 0.00 | 0.00 | 0.00 | |
| M1 Ti | 0.01 | 0.01 | 0.01 | 0.01 | 0.00 | 0.01 | 0.01 | 0.01 | 0.01 | 0.01 | 0.01 | 0.01 | 0.01 | 0.01 | 0.01 | 0.01 | 0.01 | 0.01 | 0.01 | 0.01 | 0.01 | 0.01 | 0.01 | 0.02 | 0.01 | |
| M1 Fe ³⁺ | 0.16 | 0.12 | 0.13 | 0.15 | 0.17 | 0.10 | 0.13 | 0.12 | 0.11 | 0.15 | 0.11 | 0.18 | 0.14 | 0.15 | 0.12 | 0.15 | 0.11 | 0.15 | 0.18 | 0.12 | 0.14 | 0.11 | 0.13 | 0.19 | 0.06 | |
| M1 Fe ²⁺ | 0.23 | 0.16 | 0.26 | 0.21 | 0.25 | 0.19 | 0.23 | 0.26 | 0.17 | 0.25 | 0.17 | 0.19 | 0.25 | 0.27 | 0.17 | 0.26 | 0.22 | 0.21 | 0.16 | 0.14 | 0.16 | 0.15 | 0.08 | 0.10 | | |
| M1 Cr | 0.00 | 0.00 | 0.00 | 0.00 | 0.00 | 0.00 | 0.00 | 0.00 | 0.00 | 0.00 | 0.00 | 0.00 | 0.00 | 0.00 | 0.00 | 0.00 | 0.00 | 0.00 | 0.00 | 0.00 | 0.00 | 0.00 | 0.00 | 0.00 | 0.00 | |
| M1 Mg | 0.56 | 0.71 | 0.57 | 0.62 | 0.53 | 0.70 | 0.61 | 0.59 | 0.71 | 0.57 | 0.71 | 0.60 | 0.57 | 0.56 | 0.69 | 0.55 | 0.65 | 0.61 | 0.61 | 0.68 | 0.68 | 0.70 | 0.71 | 0.67 | 0.82 | |
| M2 Fe ²⁺ | 0.00 | 0.01 | 0.00 | 0.00 | 0.00 | 0.01 | 0.00 | 0.00 | 0.01 | 0.00 | 0.00 | 0.00 | 0.00 | 0.00 | 0.00 | 0.00 | 0.00 | 0.00 | 0.00 | 0.00 | 0.00 | 0.00 | 0.00 | 0.00 | 0.02 | |
| M2 Mn | 0.04 | 0.02 | 0.03 | 0.02 | 0.05 | 0.02 | 0.03 | 0.02 | 0.03 | 0.02 | 0.03 | 0.03 | 0.02 | 0.03 | 0.03 | 0.02 | 0.03 | 0.03 | 0.03 | 0.03 | 0.02 | 0.02 | 0.02 | 0.02 | 0.01 | |
| M2 Ca | 0.88 | 0.90 | 0.89 | 0.86 | 0.90 | 0.89 | 0.90 | 0.89 | 0.91 | 0.87 | 0.91 | 0.89 | 0.92 | 0.89 | 0.89 | 0.89 | 0.90 | 0.89 | 0.89 | 0.91 | 0.91 | 0.92 | 0.91 | 0.89 | 0.93 | |
| M2 Na | 0.12 | 0.08 | 0.09 | 0.10 | 0.13 | 0.07 | 0.09 | 0.09 | 0.08 | 0.11 | 0.08 | 0.12 | 0.09 | 0.10 | 0.08 | 0.11 | 0.09 | 0.11 | 0.12 | 0.09 | 0.09 | 0.08 | 0.08 | 0.13 | 0.05 | |
| M2 K | 0.00 | 0.00 | 0.00 | 0.00 | 0.00 | 0.00 | 0.00 | 0.00 | 0.00 | 0.00 | 0.00 | 0.00 | 0.00 | 0.00 | 0.00 | 0.00 | 0.00 | 0.00 | 0.00 | 0.00 | 0.00 | 0.00 | 0.00 | 0.01 | 0.00 | |
| 计算辉石的端元组分 | | | | | | | | | | | | | | | | | | | | | | | | | | |
| Wo | 46.78 | 47.15 | 47.55 | 47.17 | 46.15 | 47.39 | 47.23 | 47.07 | 46.76 | 47.13 | 47.34 | 46.33 | 47.44 | 46.75 | 47.95 | 47.36 | 47.37 | 47.19 | 47.12 | 47.95 | 48.15 | 48.37 | 47.52 | 47.95 | 47.77 | |
| En | 29.70 | 37.15 | 30.07 | 32.57 | 28.57 | 36.61 | 32.19 | 31.36 | 37.06 | 30.30 | 36.91 | 31.88 | 29.91 | 29.28 | 35.85 | 29.29 | 34.13 | 32.30 | 32.57 | 35.94 | 35.82 | 36.40 | 37.01 | 35.95 | 42.32 | |
| Fs | 23.52 | 15.70 | 22.38 | 20.26 | 25.28 | 15.99 | 20.58 | 21.57 | 16.18 | 22.57 | 15.76 | 21.80 | 22.66 | 23.97 | 16.21 | 23.35 | 18.50 | 20.51 | 20.32 | 16.11 | 16.03 | 15.23 | 15.47 | 16.10 | 9.91 | |
| Wef | 87.67 | 92.12 | 90.48 | 89.77 | 86.66 | 92.60 | 90.33 | 90.41 | 92.27 | 88.73 | 92.34 | 87.64 | 90.64 | 89.69 | 91.86 | 88.86 | 91.33 | 88.98 | 87.47 | 91.11 | 90.42 | 92.28 | 91.90 | 86.87 | 95.10 | |
| Jd | 0.00 | 0.00 | 0.24 | 0.00 | 0.00 | 0.88 | 0.00 | 0.79 | 0.07 | 0.11 | 0.02 | 0.00 | 0.00 | 0.00 | 0.22 | 0.23 | 0.05 | 0.00 | 0.07 | 0.00 | 0.00 | 0.63 | 0.02 | 0.00 | 0.36 | |
| Ae | 12.33 | 7.89 | 9.28 | 10.23 | 13.34 | 6.53 | 9.67 | 8.80 | 7.67 | 11.16 | 7.65 | 12.36 | 9.36 | 10.31 | 8.14 | 10.92 | 8.44 | 10.97 | 12.53 | 8.81 | 9.58 | 7.09 | 8.08 | 13.13 | 4.53 | |
| Mg [#] | 58.15 | 71.57 | 59.21 | 63.18 | 55.74 | 71.01 | 62.77 | 61.08 | 71.16 | 59.14 | 71.43 | 61.05 | 58.86 | 56.83 | 70.30 | 57.52 | 66.52 | 62.86 | 63.31 | 70.49 | 70.56 | 71.88 | 71.73 | 70.36 | 81.65 | |

续表2

| 岩石类型 部位 | 黑云辉石正长岩(HS8-48) | | | | | | | | | | | | | | | | | | | | | | | | |
|--------------------------------|-----------------|-----------|-----------|-----------|----------|----------|----------|----------|----------|----------|----------|----------|----------|-----------|-----------|-----------|-----------|-----------|-----------|-----------|-----------|-----------|-----------|-----------|--|
| | 4-11 幔 | 4-12 幔 | 4-13 边 | 4-14 边 | 9-1 幔 | 9-2 幔 | 9-3 幔 | 9-4 幔 | 9-5 幔 | 9-6 幔 | 9-7 幔 | 9-8 幔 | 9-9 幔 | 9-10 幔 | 9-11 幔 | 9-12 幔 | 9-13 幔 | 9-14 幔 | 10-1 幔 | 10-2 幔 | 10-3 幔 | 10-4 幔 | 10-5 幔 | 10-6 幔 | |
| SiO ₂ | 51.30 | 51.99 | 51.62 | 51.47 | 52.42 | 52.18 | 51.04 | 51.68 | 52.82 | 52.31 | 52.52 | 51.89 | 51.69 | 52.05 | 51.45 | 52.30 | 51.71 | 51.51 | 50.97 | 52.19 | 52.31 | 51.70 | 51.50 | 51.94 | |
| TiO ₂ | 0.51 | 0.47 | 0.28 | 0.20 | 0.39 | 0.37 | 0.56 | 0.61 | 0.30 | 0.41 | 0.33 | 0.28 | 0.30 | 0.29 | 0.28 | 0.43 | 0.21 | 0.38 | 0.20 | 0.45 | 0.50 | 0.25 | 0.54 | 0.26 | |
| Al ₂ O ₃ | 2.18 | 1.44 | 1.23 | 1.24 | 1.45 | 1.38 | 2.40 | 1.98 | 1.20 | 1.43 | 1.32 | 1.16 | 1.23 | 1.26 | 1.21 | 1.47 | 1.17 | 1.35 | 1.45 | 1.39 | 1.57 | 1.50 | 2.15 | 1.24 | |
| FeO* | 9.35 | 8.77 | 11.47 | 11.66 | 9.23 | 8.99 | 10.00 | 9.30 | 8.30 | 8.76 | 9.13 | 11.39 | 11.55 | 11.84 | 12.74 | 8.85 | 12.31 | 9.19 | 13.45 | 8.95 | 8.96 | 11.41 | 9.09 | 11.78 | |
| Cr ₂ O ₃ | 0.00 | 0.00 | 0.03 | 0.01 | 0.02 | 0.00 | 0.00 | 0.01 | 0.01 | 0.02 | 0.00 | 0.00 | 0.01 | 0.00 | 0.02 | 0.00 | 0.03 | 0.00 | 0.00 | 0.00 | 0.01 | 0.03 | 0.01 | 0.01 | |
| MnO | 0.44 | 0.60 | 0.90 | 0.89 | 0.60 | 0.66 | 0.54 | 0.57 | 0.58 | 0.53 | 0.61 | 0.88 | 0.96 | 0.95 | 0.96 | 0.64 | 1.06 | 0.69 | 1.15 | 0.60 | 0.56 | 0.73 | 0.54 | 0.92 | |
| MgO | 12.36 | 12.74 | 11.00 | 10.77 | 12.69 | 12.52 | 11.93 | 12.29 | 13.16 | 12.75 | 12.47 | 11.12 | 10.81 | 10.88 | 9.95 | 12.80 | 10.12 | 12.00 | 9.35 | 12.63 | 12.56 | 11.04 | 12.57 | 10.85 | |
| CaO | 22.17 | 22.80 | 22.09 | 22.11 | 22.59 | 22.92 | 22.68 | 22.75 | 23.22 | 22.87 | 22.96 | 21.97 | 22.22 | 21.97 | 22.19 | 22.91 | 21.91 | 22.68 | 21.35 | 22.55 | 22.89 | 22.20 | 22.40 | 21.99 | |
| Na ₂ O | 1.08 | 1.04 | 1.43 | 1.41 | 1.13 | 1.04 | 1.12 | 1.17 | 0.80 | 1.06 | 1.07 | 1.38 | 1.37 | 1.36 | 1.43 | 1.05 | 1.62 | 1.05 | 1.56 | 0.98 | 1.02 | 1.25 | 1.06 | 1.25 | |
| K ₂ O | 0.05 | 0.01 | 0.00 | 0.02 | 0.02 | 0.00 | 0.00 | 0.02 | 0.00 | 0.01 | 0.01 | 0.00 | 0.01 | 0.00 | 0.01 | 0.00 | 0.02 | 0.02 | 0.11 | 0.01 | 0.00 | 0.00 | 0.00 | 0.02 | |
| Total | 99.43 | 99.85 | 100.05 | 99.77 | 100.53 | 100.06 | 100.26 | 100.38 | 100.39 | 100.13 | 100.42 | 100.07 | 100.13 | 100.59 | 100.22 | 100.46 | 100.15 | 98.88 | 99.59 | 99.75 | 100.39 | 100.10 | 99.86 | 100.27 | |
| 阳离子数(以6个氧原子计算) | | | | | | | | | | | | | | | | | | | | | | | | | |
| T Si | 1.92 | 1.94 | 1.94 | 1.94 | 1.94 | 1.94 | 1.90 | 1.92 | 1.96 | 1.94 | 1.95 | 1.94 | 1.95 | 1.94 | 1.95 | 1.94 | 1.94 | 1.95 | 1.94 | 1.95 | 1.94 | 1.94 | 1.92 | 1.95 | |
| T Al | 0.08 | 0.06 | 0.05 | 0.06 | 0.06 | 0.06 | 0.10 | 0.08 | 0.04 | 0.06 | 0.05 | 0.05 | 0.05 | 0.05 | 0.05 | 0.05 | 0.05 | 0.05 | 0.06 | 0.05 | 0.05 | 0.06 | 0.08 | 0.05 | |
| T Fe ³⁺ | 0.00 | 0.00 | 0.01 | 0.00 | 0.00 | 0.00 | 0.00 | 0.00 | 0.00 | 0.00 | 0.00 | 0.00 | 0.00 | 0.00 | 0.00 | 0.00 | 0.00 | 0.00 | 0.00 | 0.00 | 0.00 | 0.00 | 0.00 | 0.00 | |
| M1 Al | 0.02 | 0.00 | 0.00 | 0.00 | 0.01 | 0.00 | 0.01 | 0.01 | 0.01 | 0.01 | 0.01 | 0.00 | 0.00 | 0.00 | 0.00 | 0.01 | 0.01 | 0.01 | 0.01 | 0.01 | 0.01 | 0.01 | 0.01 | 0.01 | |
| M1 Ti | 0.01 | 0.01 | 0.01 | 0.01 | 0.01 | 0.01 | 0.02 | 0.02 | 0.01 | 0.01 | 0.01 | 0.01 | 0.01 | 0.01 | 0.01 | 0.01 | 0.01 | 0.01 | 0.01 | 0.01 | 0.01 | 0.02 | 0.01 | 0.01 | |
| M1 Fe ³⁺ | 0.11 | 0.11 | 0.15 | 0.11 | 0.11 | 0.14 | 0.13 | 0.07 | 0.10 | 0.10 | 0.14 | 0.14 | 0.13 | 0.15 | 0.11 | 0.16 | 0.11 | 0.16 | 0.08 | 0.09 | 0.13 | 0.11 | 0.12 | 0.25 | |
| M1 Fe ²⁺ | 0.17 | 0.16 | 0.21 | 0.17 | 0.17 | 0.16 | 0.18 | 0.17 | 0.18 | 0.22 | 0.22 | 0.24 | 0.25 | 0.16 | 0.23 | 0.19 | 0.27 | 0.19 | 0.19 | 0.23 | 0.16 | 0.25 | 0.16 | 0.25 | |
| M1 Cr | 0.00 | 0.00 | 0.00 | 0.00 | 0.00 | 0.00 | 0.00 | 0.00 | 0.00 | 0.00 | 0.00 | 0.00 | 0.00 | 0.00 | 0.00 | 0.00 | 0.00 | 0.00 | 0.00 | 0.00 | 0.00 | 0.00 | 0.00 | 0.00 | |
| M1 Mg | 0.69 | 0.71 | 0.62 | 0.61 | 0.70 | 0.66 | 0.68 | 0.73 | 0.71 | 0.69 | 0.62 | 0.61 | 0.61 | 0.56 | 0.71 | 0.57 | 0.68 | 0.53 | 0.70 | 0.70 | 0.62 | 0.70 | 0.61 | 0.61 | |
| M2 Fe ²⁺ | 0.02 | 0.00 | 0.00 | 0.00 | 0.00 | 0.00 | 0.00 | 0.00 | 0.00 | 0.00 | 0.00 | 0.00 | 0.00 | 0.00 | 0.00 | 0.00 | 0.00 | 0.00 | 0.00 | 0.00 | 0.00 | 0.00 | 0.00 | 0.00 | |
| M2 Mn | 0.01 | 0.02 | 0.03 | 0.03 | 0.02 | 0.02 | 0.02 | 0.02 | 0.02 | 0.02 | 0.03 | 0.03 | 0.03 | 0.03 | 0.03 | 0.03 | 0.03 | 0.02 | 0.04 | 0.02 | 0.02 | 0.02 | 0.02 | 0.03 | |
| M2 Ca | 0.89 | 0.91 | 0.89 | 0.90 | 0.91 | 0.91 | 0.92 | 0.91 | 0.91 | 0.88 | 0.90 | 0.88 | 0.90 | 0.91 | 0.88 | 0.92 | 0.87 | 0.90 | 0.91 | 0.89 | 0.90 | 0.89 | 0.90 | 0.89 | |
| M2 Na | 0.08 | 0.08 | 0.10 | 0.10 | 0.08 | 0.08 | 0.08 | 0.08 | 0.08 | 0.08 | 0.10 | 0.10 | 0.10 | 0.10 | 0.10 | 0.10 | 0.08 | 0.12 | 0.07 | 0.07 | 0.09 | 0.08 | 0.09 | 0.09 | |
| M2 K | 0.00 | 0.00 | 0.00 | 0.00 | 0.00 | 0.00 | 0.00 | 0.00 | 0.00 | 0.00 | 0.00 | 0.00 | 0.00 | 0.00 | 0.00 | 0.00 | 0.00 | 0.00 | 0.01 | 0.00 | 0.00 | 0.00 | 0.00 | 0.00 | |
| 计算辉石的端元组分 | | | | | | | | | | | | | | | | | | | | | | | | | |
| Wo | 47.16 | 47.65 | 46.94 | 47.15 | 47.14 | 47.87 | 47.74 | 47.91 | 47.77 | 46.73 | 47.24 | 46.65 | 47.47 | 47.59 | 47.18 | 48.16 | 46.65 | 47.39 | 47.88 | 47.19 | 47.25 | 46.77 | | | |
| En | 36.58 | 37.05 | 32.53 | 31.94 | 36.84 | 36.39 | 34.93 | 35.95 | 37.78 | 37.06 | 36.20 | 32.90 | 31.97 | 32.14 | 29.63 | 37.01 | 30.32 | 35.45 | 28.43 | 36.94 | 36.56 | 32.66 | 36.90 | 32.12 | |
| Fs | 16.26 | 15.29 | 20.53 | 20.91 | 16.02 | 15.74 | 17.33 | 16.21 | 14.31 | 15.17 | 15.88 | 20.37 | 20.79 | 21.21 | 22.91 | 15.40 | 22.50 | 16.39 | 24.92 | 15.68 | 15.56 | 20.15 | 15.86 | 21.12 | |
| Wef | 91.90 | 92.28 | 89.29 | 89.43 | 91.70 | 92.30 | 91.57 | 91.28 | 94.14 | 92.21 | 92.12 | 89.73 | 89.78 | 89.87 | 89.30 | 92.27 | 87.89 | 92.11 | 88.10 | 92.79 | 92.46 | 90.63 | 92.06 | 90.69 | |
| Jd | 1.13 | 0.06 | 0.00 | 0.00 | 0.34 | 0.28 | 0.40 | 0.35 | 0.66 | 0.45 | 0.53 | 0.00 | 0.00 | 0.28 | 0.00 | 0.11 | 0.00 | 0.37 | 0.43 | 0.85 | 0.77 | 0.56 | 0.89 | 0.53 | |
| Ae | 6.97 | 7.65 | 10.71 | 10.57 | 7.96 | 7.43 | 8.04 | 8.38 | 5.20 | 7.34 | 7.35 | 10.27 | 10.23 | 9.85 | 10.70 | 7.62 | 12.11 | 7.52 | 11.47 | 6.35 | 6.76 | 8.81 | 7.05 | 8.77 | |
| Mg [#] | 70.21 | 72.14 | 63.09 | 62.20 | 71.03 | 71.29 | 68.02 | 70.21 | 73.87 | 72.18 | 70.87 | 63.51 | 62.51 | 62.08 | 58.20 | 72.05 | 59.44 | 69.94 | 55.35 | 71.56 | 71.42 | 63.30 | 71.15 | 62.14 | |

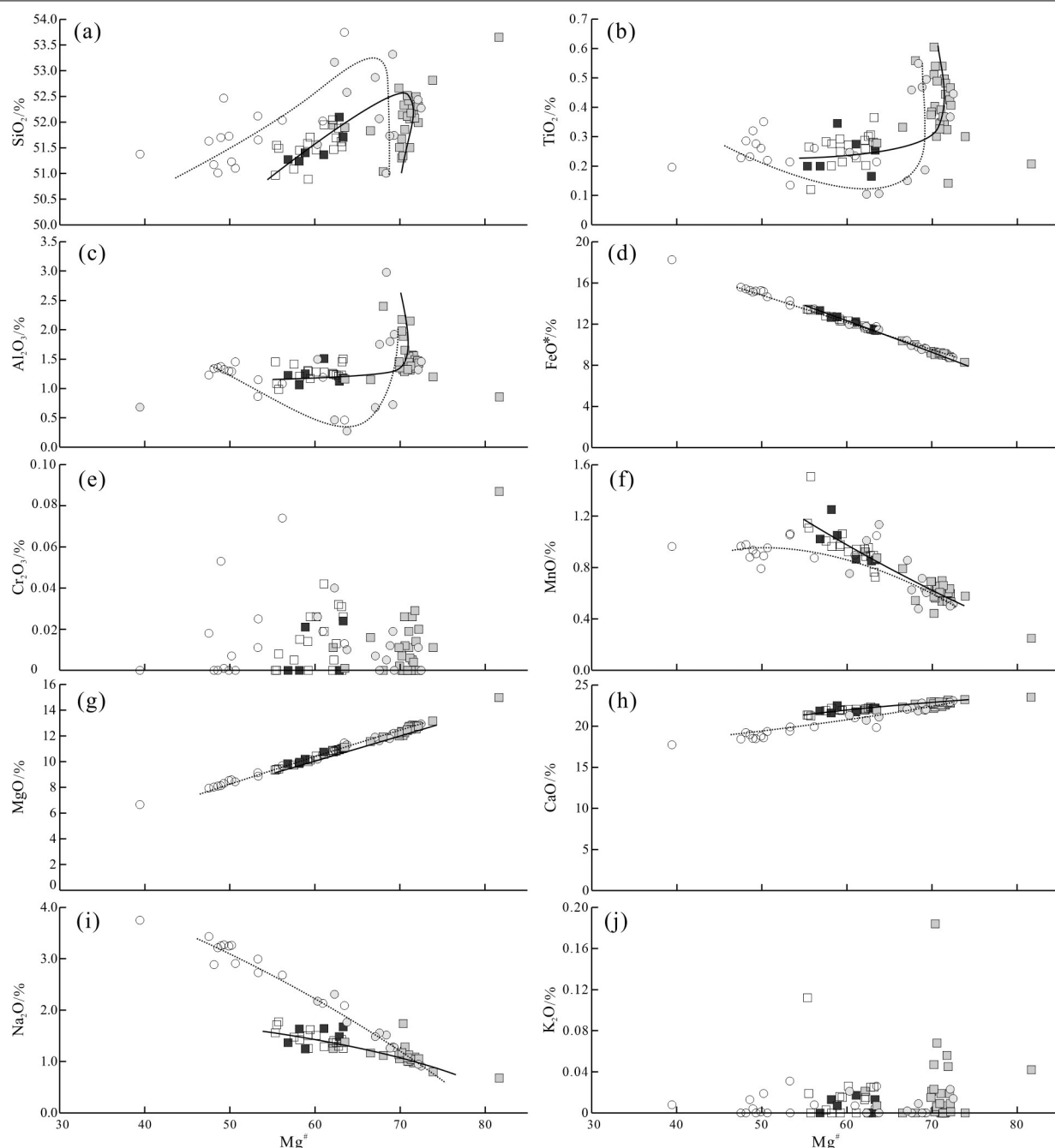


图7 洪山正长岩杂岩体单斜辉石各组分与Mg[#]之间的相关图解(图例同图6)

Fig. 7 Correlation diagrams of chemical composition versus Mg[#] for clinopyroxene from the Hongshan syenite complex
(symbols as for Fig. 6)

所有数据点投在Wo–En–Fs三角图中(图6b),所有Cpx几乎全部落入次透辉石和铁普通辉石区域;将所有数据点投在WEF–Jd–Ae三角图中(图6c),所有点均位于Ca–Mg–Fe和霓石–普通辉石区域。通过投图可以发现,黑云辉石正长岩中几乎所有Cpx(不论核部、幔部还是边部)均为Ca–Mg–Fe系列的

次透辉石,辉石正长岩中Cpx核部均为Ca–Mg–Fe系列的次透辉石区域,而边部位于铁普通辉石和Ca–Na系列的霓石–普通辉石区域。

在单斜辉石Mg[#]值哈克图解上(图7),Mg[#]值与SiO₂、TiO₂、Al₂O₃、MgO、CaO呈现出较好的正相关关系,与FeO*、MnO、Na₂O则呈现出较好的负相关关

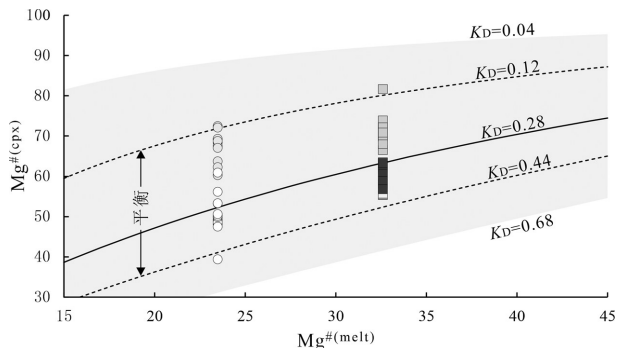


图8 洪山正长岩杂岩体单斜辉石罗德图(据Rhodes et al., 1979; Di et al., 2020修改, 图例同图6)

Fig. 8 Rhodes diagram for clinopyroxenes form the Hongshan syenite complex (modified from Rhodes et al., 1979; Di et al., 2020, symbols as for Fig. 6)

系,与 Cr_2O_3 、 K_2O 相关性不明显。除与 $\text{Mg}^{\#}$ 值直接相关的 FeO^* 和 MgO 外,其余与单斜辉石 $\text{Mg}^{\#}$ 值相关性较好的几种氧化物中,辉石正长岩与黑云辉石正长岩中Cpx的趋势并不相同,表现为辉石正长岩中Cpx的核部与黑云辉石正长岩中Cpx的幔部具有一致的元素含量特征,并且变化范围较小,而辉石正长岩中Cpx的边部与黑云辉石正长岩中Cpx的核部、边部元素含量明显不同,并且变化范围较大。

单斜辉石及其与之平衡的熔体间 Fe 与 Mg 有 $[K_D(\text{Fe}-\text{Mg})]^{\text{Cpx}-\text{melt}} = (\text{Fe}/\text{Mg})^{\text{Cpx}}/(\text{Fe}/\text{Mg})^{\text{melt}}$,其中 Fe 与 Mg 都是摩尔含量]的平衡公式,Putirka (2008)利用1245个实验观测值得到 K_D 大致在0.04~0.68间的正态分布范围,平均值为0.28($1\sigma=0.08$),使用该标准在 $2\sigma=0.16$ 时,可以得到 K_D 在0.12~0.44的平衡区间(图8)。本文所有测试点几乎位于 $K_D=0.12\sim0.44$ 范围内,说明单斜辉石与熔体已达平衡状态,不太可能存在捕虏晶的情况(Di et al., 2020),结合单斜辉石具有清晰界线的核-边或者核-幔-边结构,可能是流体改造的结果。

5 讨 论

5.1 黑云辉石正长岩形成时代

黑云辉石正长岩中锆石CL图像显示其发育振荡环带,具有相对较高的 Th/U 比值,表现出了岩浆锆石的特征,其测定的年龄应该代表了岩浆的结晶年龄。黑云辉石正长岩的锆石 $^{206}\text{Pb}/^{238}\text{U}$ 年龄分别为123.9~132.3 Ma,其加权平均年龄为(126.9 ± 1.2) Ma

(1σ , MSWD=1.07, $n=15$),表明其形成时代为早白垩世,暗示了洪山正长岩杂岩体形成时代与华北克拉通岩石圈减薄的峰期年龄相一致(Zhai et al., 2004; 吴福元等, 2008; Xu et al., 2009; Zhu et al., 2011, 2012a, b; Zheng et al., 2018; Wang et al., 2018; Zhu and Xu, 2019),并与华北克拉通其他中生代富碱性杂岩体形成时代一致(例如: Yan et al., 2000; Zhang et al., 2005; 吴福元等, 2005; 阎国翰等, 2007; Yang et al., 2009; 陈春良等, 2014; 段友强等, 2015; 王亚莹等, 2015; 霍腾飞等, 2016; Sun et al., 2019)。这一年龄与洪山正长岩杂岩体辉石正长岩年龄(125.6 ± 1.2) Ma(未发表数据)一致,并略早于辉石正长岩的形成年龄,其年龄的微小差异与洪山正长岩杂岩体相带分布特征吻合。

5.2 洪山正长岩杂岩体中单斜辉石结晶趋势及岩浆体系特征

洪山正长岩杂岩体中Cpx与Shonkin Sag岩体中Cpx类似,总体具有透辉石→霓石的演化趋势(图6b),但辉石正长岩Cpx核部、黑云辉石正长岩Cpx与河北矾山杂岩体中Cpx类似,均具有较高的 CaO 含量(牛晓露等, 2009),其 $\text{Ca}/(\text{Ca}+\text{Mg}+\text{Fe})$ 分别介于46.1~51.7、48.2~52.1,比Shonkin Sag岩体的初始演化趋势高(图6b, Nash and Wilkinson, 1970),表现为Cpx具有更高的 Ca^{2+} 含量,并具有次透辉石→铁次透辉石方向的近水平演化趋势,表明Cpx结晶早期,有 Fe^{2+} 对 Mg^{2+} 的取代关系;而辉石正长岩中Cpx边部在透辉石→霓石的演化趋势下方,暗示了此时 Ca^{2+} 含量变低,更多地被 Fe^{2+} 、 Fe^{3+} 和 Na^{+} 取代,说明岩浆是向更加富铁、钠的方向演化的(图6)。这样的趋势反映了岩浆体系具有高温、中等氧逸度(Aoki, 1964; Gibb, 1973; 邱家骥和廖群安, 1996)和富碱(尤其是富钠)的特点。

5.3 洪山正长岩杂岩体中单斜辉石的形成过程

大量研究表明,Cpx的成分主要受母岩浆的成分与结晶环境的制约(Le Bas, 1962; 邱家骥和廖群安, 1996; 白志民, 2000; Gao et al., 2008; 牛晓露等, 2009, 2016; Chen et al., 2018; 刘鑫和汤艳杰, 2018),其成分可以很好地反映母岩浆的成分特征。通过观察黑云辉石正长岩与辉石正长岩中Cpx主量元素含量(表2),可以发现黑云辉石正长岩中Cpx幔部与辉石正长岩中Cpx核部具有较为一致的主量元素含

量,结合Mg[#]值哈克图解(图7)演化趋势,可以清楚地发现黑云辉石正长岩中Cpx幔部与辉石正长岩中Cpx核部集中在较小的范围变化(图7a-c,f,h,i),说明它们结晶过程中可能具有相同的母岩浆成分,并且结晶环境较为稳定,形成了差别较小、无环带特征的Cpx。

黑云辉石正长岩与辉石正长岩中Cpx的边部成分差异较大,说明了Cpx边部在结晶过程中,辉石正长岩与黑云辉石正长岩经历了不同的演化过程,表现为辉石正长岩中Cpx边部结晶时母岩浆更加富硅、铁、钠(图7a,d,i),贫钛、铝、锰、镁、钙(图7b,c,f,g,h),尤其以铁、钠含量差别明显(图7d,i),使得辉石正长岩中Cpx边部向霓石-普通辉石方向演化(图6b,c),结合采样位置(图2),辉石正长岩位于洪山正长岩杂岩体中部,靠近中心相的正长岩,而这里结晶相对较晚,反映了晚期岩浆残余成分演化的过程,随着结晶过程的进行,岩浆向着富铁、富碱的方向演化,这也表现在Cpx边缘发育较多的磁铁矿(图5),而仅仅通过岩浆演化,在连续的结晶过程中并不会形成Cpx核部与边部截然的接触关系(图5),辉石分类图解中辉石正长岩中Cpx核部与边部成分变化也是不连续的(图6a,c),Mg[#]值哈克图解和罗德图中同样反映了不连续的演化过程(图7、图8),并且辉石正长岩中钾长石边缘发育钠长石反应边(图3b)等特征,说明除了岩浆自身的演化外,洪山正长岩杂岩体中部还经历了一次富钠、富铁流体的作用,流体对辉石正长岩的作用强度明显大于对黑云辉石正长岩的作用强度(图9),说明富钠、富铁流体可能由西向东(或者由洪山正长岩杂岩体中部向外部)对杂

岩体进行改造的。

6 结 论

通过对洪山正长岩杂岩体野外调查研究,以及辉石正长岩、黑云辉石正长岩中单斜辉石、锆石LA-ICP-MS U-Pb年代学研究,可以得出以下结论:

(1)洪山正长岩杂岩体黑云辉石正长岩加权平均年龄分别为(126.9 ± 1.2)Ma(1σ , MSWD=1.07, $n=15$),是早白垩世华北克拉通减薄峰期的产物。

(2)洪山正长岩杂岩体中单斜辉石总体具有透辉石→霓石的演化趋势,初始演化时具有Fe²⁺对Mg²⁺的取代关系,随着演化的进行,岩浆更加富铁、富钠,反映了岩浆体系具有高温、中等氧逸度和富碱(尤其是富钠)的特点。

(3)洪山正长岩杂岩体形成后,可能受到了由西向东(或者由洪山正长岩杂岩体中部向外部)的富钠、富铁流体的改造。

注释

①赵祯祥,杜晋峰,段春森. 2008. 长治市幅J49C004004 1:25万区域地质调查报告[R]. 太原: 山西省地质调查院.

②张兆伟,杨红宾,徐永利,靳松,赵保强,樊延恩,王建武,王克冰,李锋,孙阳,胡建忠,王健宇,毕立. 2014. 邯郸市幅J50C004001 1:25万区域地质调查报告[R]. 石家庄: 河北省地质调查院.

References

- Andersen T. 2002. Correction of common lead in U-Pb analyses that do not report ^{204}Pb [J]. Chemical Geology, 192(1/2): 59–79.
- Aoki K I. 1964. Clinopyroxenes from alkaline rocks of Japan[J]. American Mineralogist: Journal of Earth and Planetary Materials, 49(9/10): 1199–1223.
- Bai Zhimin. 2000. Mineral chemistry and genetic significance of clinopyroxenes from the Mesozoic volcanic rocks in Western Hills of Beijing[J]. Acta Petrologica et Mineralogica, 19(2): 174–184 (in Chinese with English abstract).
- Chen B, Tian W, Jahn B M, Chen Z C. 2008. Zircon SHRIMP U-Pb ages and in-situ Hf isotopic analysis for the Mesozoic intrusions in South Taihang, North China craton: Evidence for hybridization between mantle-derived magmas and crustal components[J]. Lithos, 102(1/2): 118–137.
- Chen Chunliang, Jiang Sihong, Liang Qingling, Liu Yuan, Han Ning. 2014. The Hf isotopic characteristics of the zircons from Wulingshan complex in Hebei and regional comparative study[J]. Geoscience, 28(4): 663–673 (in Chinese with English abstract).
- Chen L, Zheng Y F, Zhao Z F. 2018. Geochemical insights from

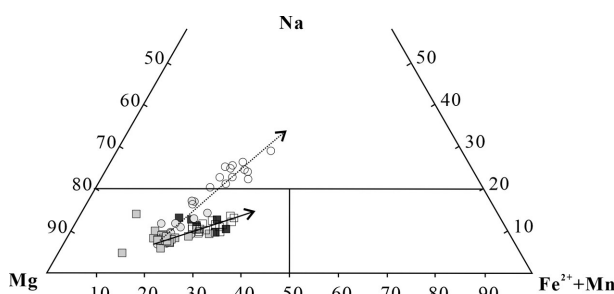


图9 洪山正长岩杂岩体单斜辉石Mg-Na-(Fe²⁺+Mn)图解
(据Eby et al., 1998修改, 图例同图6)

Fig. 9 Mg-Na-(Fe²⁺+Mn) diagram for clinopyroxenes from the Hongshan syenite complex (modified from Eby et al., 1998, symbols as for Fig. 6)

- clinopyroxene phenocrysts into the effect of magmatic processes on petrogenesis of intermediate volcanics[J]. *Lithos*, 316: 137–153.
- Deng X D, Li J W, Wen G. 2015. U–Pb geochronology of hydrothermal zircons from the early Cretaceous iron skarn deposits in the Handan–Xingtai district, North China craton [J]. *Economic Geology*, 110(8): 2159–2180.
- Di Y K, Tian W, Chen M M, Li Z F, Chu Z Y, Liang J. 2020. A method to estimate the pre-eruptive water content of basalts: Application to the Wudalianchi–Erkeshan–Kelu volcanic field, Northeastern China[J]. *American Mineralogist: Journal of Earth and Planetary Materials*, 105(2): 149–161.
- Dobosi G, Fodor R V. 1992. Magma fractionation, replenishment, and mixing as inferred from green–core clinopyroxenes in Pliocene basanite, southern Slovakia[J]. *Lithos*, 28(2): 133–150.
- Duan Youqiang, Zhang Zhengwei, Yang Xiaoyong. 2015. The continental dynamics of Zhangshiyang pluton at the southern margin of the North China Craton: Evidence from geochemical, zircon U–Pb geochronology and Hf isotopic compositions[J]. *Acta Petrologica Sinica*, 31(7): 1995–2008 (in Chinese with English abstract).
- Eby G N, Woolley A R, Din V, Platt G. 1998. Geochemistry and petrogenesis of nepheline syenites: Kasungu–Chipala, Ilomba, and Ulini nepheline syenite intrusions, North Nyasa alkaline province, Malawi[J]. *Journal of Petrology*, 39(8): 1405–1424.
- Huang Xiaolong, Xu Yigang, Yang Qijun, Chen Linli. 2007. Genesis of compositional zoning of clinopyroxene phenocrysts in the Wozhong Late Eocene high–Mg ultrapotassic lavas, western Yunnan, China: Magma replenishment–mixing process[J]. *Geological Journal of China Universities*, 13(2): 250–260 (in Chinese with English abstract).
- Huo Tengfei, Yang Debin, Shi Jiangpeng, Xu Wenliang, Yang Haotian. 2016. Petrogenesis of the Early Cretaceous alkali-rich intrusive rocks in the central North China Block: Constraints from zircon U–Pb chronology and Sr–Nd–Hf isotopes[J]. *Acta Petrologica Sinica*, 32(3): 697–712 (in Chinese with English abstract).
- Gao S, Rudnick R L, Xu W L, Yuan H L, Liu Y S, Walker R J, Puchtel I S, Liu X M, Huang H, Wang X R, Yang J. 2008. Recycling deep cratonic lithosphere and generation of intraplate magmatism in the North China Craton[J]. *Earth and Planetary Science Letters*, 270(1/2): 41–53.
- Gao S, Rudnick R L, Yuan H L, Liu X M, Liu Y S, Xu W L, Ling W L, Ayers J, Wang X C, Wang Q H. 2004. Recycling lower continental crust in the North China craton[J]. *Nature*, 432(7019): 892–897.
- Gibb F G F. 1973. The zoned clinopyroxenes of the Shiant Isles sill, Scotland[J]. *Journal of Petrology*, 14(2): 203–230.
- Goleń M, Puziewicz J, Matusiak–Małek M, Ntaflos T. 2015. Clinopyroxene phenocrysts from the Księginki nephelinite (SW Poland) [J]. *Geoscience Records*, 1(1/2): 1–15.
- Jiang Shaoyong, Zhao Kuidong, Jiang Yaohui, Ling Hongfei, Ni Pei. 2006. New type of tin mineralization related to granite in South China: Evidence from mineral chemistry, element and isotope geochemistry[J]. *Acta Petrologica Sinica*, 22(10): 2509–2516 (in Chinese with English abstract).
- Jiang Shaoyong, Li Liang, Zhu Bi, Ding Xin, Jiang Yaohui, Gu Lianxing, Ni Pei. 2008. Geochemical and Sr–Nd–Hf isotopic compositions of granodiorite from the Wushan copper deposit, Jiangxi Province and their implications for petrogenesis[J]. *Acta Petrologica Sinica*, 24(8): 1679–1690 (in Chinese with English abstract).
- Le Bas M J. 1962. The role of aluminum in igneous clinopyroxenes with relation to their parentage[J]. *American Journal of Science*, 260(4): 267–288.
- Li Suimin, Li Yucheng, Zhao Shumei, Zhang Liangliang, Wang Junge, Han Tengfei, Sun Zhiwei, Han Yuchou, Li Tong. 2020. Ar–Ar and U–Pb ages of Hongshan copper deposit, Handan and their limitation on mineralization time [J/OL]. *Geology in China*, [2020–02–04]: 1–17 (in Chinese with English abstract).
- Liu Xin, Tang Yanjie. 2018. The characteristics and implication of the zonation in clinopyroxene phenocrysts from the Yaojiazhuang ultramafic–syenitic complex, northwestern Hebei Province[J]. *Acta Petrologica Sinica*, 34(11): 3315–3326 (in Chinese with English abstract).
- Luo Zhaohua, Deng Jinfu, Han Xiuqing. 1999. Characteristics of Magmatic Activities and Orogenic Process of Taihangshan Intraplate Orogen[M]. Beijing: Geological Publishing House, 1–132 (in Chinese).
- Ludwig K R. 2003. ISOPLOT 3.0: A geochronological toolkit for Microsoft Excel[J]. Berkeley Geochronology Center Special Publications, 4.
- Marks M, Halama R, Wenzel T, Markl G. 2004. Trace element variations in clinopyroxene and amphibole from alkaline to peralkaline syenites and granites: Implications for mineral–melt trace-element partitioning[J]. *Chemical Geology*, 211(3/4): 185–215.
- Morimoto N. 1988. Nomenclature of pyroxenes[J]. *Mineralogy and Petrology*, 39(1): 55–76.
- Nash W P, Wilkinson J F G. 1970. Shonkin Sag Laccolith, Montana[J]. *Contributions to Mineralogy and Petrology*, 25(4): 241–269.
- Niu Xiaolu, Chen Bin, Ma Xu. 2009. Clinopyroxenes from the Fanshan pluton, Hebei[J]. *Acta Petrologica Sinica*, 25(2): 359–373 (in Chinese with English abstract).
- Putirka K D. 2008. Thermometers and barometers for volcanic systems[J]. *Reviews in mineralogy and geochemistry*, 69(1): 61–120.
- Qiu Jiaxiang, Liao Qunan. 1987. The main characteristics and petrological significance of low pressure clinopyroxenes in the Cenozoic basalts from eastern China[J]. *Acta Petrologica Sinica*, 3(4): 1–9 (in Chinese with English abstract).

- Rhodes J M, Dungan M A, Blanchard D P, Long P E. 1979. Magma mixing at mid-ocean ridges: evidence from basalts drilled near 22° N on the Mid-Atlantic Ridge[J]. *Tectonophysics*, 55(1/2): 35–61.
- Su Shangguo, Jian Dongchuan, Xie Yuchun, Luo Zhaohua, Jiang Junyi, Liu Lulu, Huo Yanan, Cui Xiaoliang, Zhang Bo, Gu Dapeng, Wang Yu. 2017. The practice of thematic geological mapping in medium-large scale for intermediate-basic intrusive rocks: A case study of the Wu'an iron ore concentration area, Hebei Province[J]. *Geological Bulletin of China*, 36(11): 1987–1998(in Chinese with English abstract).
- Sun J F, Zhang J H, Yang J H, Yang Y H, Chen S. 2019. Tracing magma mixing and crystal–melt segregation in the genesis of syenite with mafic enclaves: Evidence from in situ zircon Hf–O and apatite Sr–Nd isotopes[J]. *Lithos*, 334: 42–57.
- Wang Y, Sun L X, Zhou L Y, Xie Y T. 2018. Discussion on the relationship between the Yanshanian Movement and cratonic destruction in North China[J]. *Science China (Earth Sciences)*, 61: 499–514.
- Wang Yaying, Cai Jianhui, Yan Guohan, Yan Zhijiao, Song Jianqiang. 2015. Geochemistry and mineral characteristics of Zijinshan alkaline complex from Linxian, Shanxi Province and its Petrogenesis[J]. *Geoscience*, 29(4): 896–911 (in Chinese with English abstract).
- Wu Fuyuan, Xu Yigang, Gao Shan, Zheng Jianping. 2008. Lithospheric thinning and destruction of the North China Craton[J]. *Acta Petrologica Sinica*, 24(6): 1145–1174(in Chinese with English abstract).
- Wu Fuyuan, Yang Jinhui, Liu Xiaoming. 2005. Geochronological framework of the Mesozoic granitic magmatism in the Liaodong Peninsula, Northeast China[J]. *Geological Journal of China Universities*, 11(3): 305–317(in Chinese with English abstract).
- Xu Wenliang, Yang Chenghai, Yang Debin, Pei Fuping, Wang Qinghai, Ji Weiqiang. 2006. Mesozoic high-Mg diorites in eastern North China craton: Constraints on the mechanism of lithospheric thinning[J]. *Earth Science Frontiers*, 13(2): 120–129(in Chinese with English abstract).
- Xu Wenliang, Yang Debin, Pei Fuping, Yu Yang. 2009. Petrogenesis of Fushan high-Mg[#] diorites from the southern Taihang Mts. in the central North China Craton: Resulting from interaction of peridotite–melt derived from partial melting of delaminated lower continental crust[J]. *Acta Petrologica Sinica*, 25(8): 1947–1961(in Chinese with English abstract).
- Xu Y G, Li H Y, Pang C J, He B. 2009. On the timing and duration of the destruction of the North China Craton[J]. *Chinese Science Bulletin*, 54(19): 3379–3396.
- Yan Guohan, Cai Jianhui, Ren Kangxu, He Guoqi, Mou Baolei, Xu Baoliang, Li Fengtang, Yang Bin. 2007. Intraplate extensional magmatism of North China Craton and break-up of three supercontinents and their deep dynamics[J]. *Geological Journal of China Universities*, 13(02):161–174(in Chinese with English abstract).
- Yan G H, Xu B L, Mu B L, Wang G Y, Chang Z S, Chen T L, Zhao Y C, Wang X F, Zhang R H, Qiao G S, Chu Z Y. 2000. Alkaline intrusives at the east foot of the Taihang–Da Hinggan Mountains: Chronology, Sr, Nd and Pb isotopic characteristics and their implications[J]. *Acta Geologica Sinica*, 74(4): 774–780.
- Yang H J, Frey F A, Clague D A, Garcia M O. 1999. Mineral chemistry of submarine lavas from Hilo Ridge, Hawaii: implications for magmatic processes within Hawaiian rift zones[J]. *Contributions to Mineralogy and Petrology*, 135(4): 355–372.
- Yang X K, Chao H X, Volkova N I, Zheng M L, Yao W H. 2009. Geochemistry and SHRIMP geochronology of alkaline rocks of the Zijinshan massif in the eastern Ordos basin, China[J]. *Russian Geology and Geophysics*, 50(9): 751–762.
- Yang Zhaoyao, Xu Yaoming, Zhu Zhiyong, Zhou Wei, Bai Cheng. 2015. Mineral chemistry of pyroxene in lamprophyre from the Nangang prospecting area in the Jiurui ore district of Jiangxi Province: Implication for magma evolution[J]. *Acta Petrologica Sinica*, 31(3): 675–685(in Chinese with English abstract).
- Yuan H L, Gao S, Liu X M, Li H M, Günther D, Wu F Y. 2004. Accurate U–Pb age and trace element determinations of zircon by laser ablation–inductively coupled plasma–mass spectrometry[J]. *Geostandards and Geoanalytical Research*, 28(3): 353–370.
- Zhang Bo, Su Shangguo, Mo Xuanxue, Feng Shaochong, Wu Yue, Jiang Xiao, Feng Yanfang, Liu Jiangtao. 2020. Magmatic response to lithospheric thinning of the North China Craton: Evidence from porphyritic aegirite-bearing syenite in Wuan, Hebei, China[J/OL]. *Earth Science Frontiers*, [2020–01–22]: 1–14 (in Chinese with English abstract).
- Zhang H F, Sun M, Zhou X H, Ying J F. 2005. Geochemical constraints on the origin of Mesozoic alkaline intrusive complexes from the North China Craton and tectonic implications[J]. *Lithos*, 81(1/4): 297–317.
- Zhai M G, Zhu R X, Liu J M, Meng Q R, Hou Q L, Hu S B, Liu W, Li Z, Zhang H F, Zhang H F. 2004. Time range of Mesozoic tectonic regime inversion in eastern North China Block[J]. *Science in China Series D: Earth Sciences*, 47(2):57–65.
- Zhao G C, Sun M, Wilde S A, Li S Z. 2005. Late Archean to Paleoproterozoic evolution of the North China Craton: Key issues revisited[J]. *Precambrian Research*, 136(2): 177–202.
- Zheng Y F, Xu Z, Zhao Z F, Dai L Q. 2018. Mesozoic mafic magmatism in North China: Implications for thinning and destruction of cratonic lithosphere[J]. *Science China Earth Sciences*, 61(4): 353–385.
- Zou Jinxi, Liu Xianfan, Deng Jianghong, Deng Jianghong, Li Chunhui, Huang Yupeng, Dong Yi, Yi Liwen. 2012. Mineralogical composition characteristics and geological significance of the clinopyroxene from ultrabasic–basic rocks at Luoji village,

- Shangri-La County, Yunnan Province[J]. Acta Petrologica et Mineralogica, 31(5): 701–711 (in Chinese with English abstract).
- Zhu R X, Chen L, Wu F Y, Liu J L. 2011. Timing, scale and mechanism of the destruction of the North China Craton[J]. Science China (Earth Sciences), 54(6): 789–797.
- Zhu R X, Xu Y G. 2019. The subduction of the west Pacific plate and the destruction of the North China Craton[J]. Science China Earth Sciences, 62(9): 1340–1350.
- Zhu R X, Xu Y G, Zhu G, Zhang H F, Xia Q K, Zheng T Y. 2012a. Destruction of the North China Craton[J]. Science China (Earth Sciences), 55(10): 1565–1587.
- Zhu R X, Yang J H, Wu F Y. 2012b. Timing of destruction of the North China Craton[J]. Lithos, 149: 51–60.

附中文参考文献

- 白志民. 2000. 北京西山中生代火山岩中单斜辉石矿物化学及成因意义[J]. 岩石矿物学杂志, (2): 174–184.
- 陈春良, 江思宏, 梁清玲, 刘源, 韩宁. 2014. 河北雾灵山杂岩体锆石Hf同位素特征及其区域对比研究[J]. 现代地质, 28(4): 663–673.
- 段友强, 张正伟, 杨晓勇. 2015. 华北克拉通南缘张士英岩体大陆动力学背景:来自地球化学, 锆石U-Pb年龄和Hf同位素的证据[J]. 岩石学报, 31(7): 1995–2008.
- 黄小龙, 徐义刚, 杨启军, 陈林丽. 2007. 滇西禹中晚始新世高镁富钾火山岩中单斜辉石斑晶环带结构的成因:岩浆补给–混合过程[J]. 高校地质学报, (2): 250–260.
- 霍鹏飞, 杨德彬, 师江朋, 许文良, 杨浩田. 2016. 华北地块中部早白垩世富碱侵入岩的成因: 锆石U-Pb年代学和Sr-Nd-Hf同位素制约[J]. 岩石学报, 32(3): 697–712.
- 蒋少涌, 赵葵东, 姜耀辉, 凌洪飞, 倪培. 2006. 华南与花岗岩有关的一种新类型的锡成矿作用: 矿物化学, 元素和同位素地球化学证据[J]. 岩石学报, 22(10): 2509–2516.
- 蒋少涌, 李亮, 朱碧, 丁昕, 姜耀辉, 顾连兴, 倪培. 2008. 江西武山铜矿区花岗闪长斑岩的地球化学和Sr-Nd-Hf同位素组成及成因探讨[J]. 岩石学报, 24(8): 1679–1690.
- 李随民, 李玉成, 赵淑梅, 张良良, 王俊革, 韩鹏飞, 孙志伟, 韩玉丑, 李樞. 2020. 邯郸洪山铜矿Ar-Ar和U-Pb年龄及其对成矿时代的限定[J/OL]. 中国地质, [2020-02-04]: 1–17.
- 刘鑫, 汤艳杰. 2018. 冀西北姚家庄超镁铁岩–正长岩杂岩体中辉石的环带特征及意义[J]. 岩石学报, 34(11): 3315–3326.
- 罗照华, 邓晋福, 韩秀卿. 1999. 太行山造山带岩浆活动及其造山过程反演[M]. 北京: 地质出版社, 1–132.
- 牛晓露, 陈斌, 马旭. 2009. 河北矾山杂岩体中单斜辉石的研究[J]. 岩石学报, 25(2): 359–373.
- 邱家骥, 廖群安. 1996. 浙闽新生代玄武岩的岩石成因学与Cpx矿物化学[J]. 火山地质与矿产, 17(1): 16–25.
- 苏尚国, 简东川, 谢玉淳, 罗照华, 蒋俊毅, 刘璐璐, 霍延安, 崔晓亮, 张波, 顾大鹏, 王玉. 2017. 中基性侵入岩中一大比例尺专题地质填图实践——以河北武安铁矿集区填图试点为例[J]. 地质通报, 36(11): 1987–1998.
- 王亚莹, 蔡剑辉, 阎国翰, 闫志娇, 宋建强. 2015. 山西临县紫金山岩体地球化学、矿物学特征及岩体成因[J]. 现代地质, 29(4): 896–911.
- 吴福元, 杨进辉, 柳小明. 2005. 辽东半岛中生代花岗质岩浆作用的年代学格架[J]. 高校地质学报, 11(3): 305–317.
- 吴福元, 徐义刚, 高山, 郑建平. 2008. 华北岩石圈减薄与克拉通破坏研究的主要学术争论[J]. 岩石学报, 24(6): 1145–1174.
- 许文良, 杨承海, 杨德彬, 裴福萍, 王清海, 纪伟强. 2006. 华北克拉通东部中生代高Mg闪长岩——对岩石圈减薄机制的制约[J]. 地学前缘, 13(2): 120–129.
- 许文良, 杨德彬, 裴福萍, 于洋. 2009. 太行山南段符山高镁闪长岩的成因——拆沉陆壳物质熔融的熔体与地幔橄榄岩反应的结果[J]. 岩石学报, 25(8): 1947–1961.
- 阎国翰, 蔡剑辉, 任康绪, 何国琦, 牟保磊, 许保良, 李凤棠, 杨斌. 2007. 华北克拉通板内拉张性岩浆作用与三个超大陆裂解及深部地球动力学[J]. 高校地质学报, 13(2): 161–174.
- 杨照耀, 徐耀明, 朱志勇, 周巍, 柏成. 2015. 江西九瑞矿集区南港成矿远景区煌斑岩中辉石矿物成分特征与岩浆演化过程[J]. 岩石学报, 31(3): 675–685.
- 张波, 苏尚国, 莫宣学, 冯少憧, 伍月, 蒋校, 冯艳芳, 刘江涛. 2020. 华北克拉通减薄的岩浆岩响应:来自河北武安洪山含霓石斑状正长岩的证据[J/OL]. 地学前缘, [2020-01-22]: 1–14.
- 邹金汐, 刘显凡, 邓江红, 邓江红, 李春辉, 黄玉蓬, 董毅, 易立文. 2012. 云南香格里拉洛吉乡基性–超基性岩中单斜辉石矿物成分特征及其地质意义[J]. 岩石矿物学杂志, 31(5): 701–711.